geosciences

MDPI

Supporting Information for

Integrating Seismic Methods for Characterizing and Monitoring Landslides: A Case Study of the Heinzenberg Deep-Seated Gravitational Slope Deformation (Switzerland)

Franziska Glueer[1*], Anne-Sophie Mreyen[2], Lena Cauchie[2], Hans-Balder Havenith[2], Paolo Bergamo[1], Miroslav Halló[1] and Donat Fäh[1]

[1] Swiss Seismological Service, ETH Zürich, Zurich, Switzerland;
[2] University of Liege, 4000 Liege, Belgium;
* Correspondence: franziska.glueer@sed.ethz.ch);

Contents of this file

Figures S1 to S30.

Introduction

This supporting information file shows results of the seismic analysis regarding polarization analysis (S1 – S5), H/V spectral ratios (S6), SRT profiles (S7 – S12), used dispersion curves for all arrays (S13 – S19) and results of the joint inversion of dispersion curves by Neopsy (S20 – S30).

Figures S1 – S5 show the polarization analysis results for selected stations of the presented arrays: the parameters of the polarization, i.e. the particle motion ellipticity, the dip, and the strike. Figures S6 shows the H/V curves by the classic (left panels) and raydec (right panels) methods for selected stations of the presented arrays. Figs. S7 – S12 show the location and results of the SRT profiles SP01 to SP07 with shots on each end of the profile with two color scale solutions per profile. The outcome of each processing technique applied for the analysis of our array data and the dispersion curves picked for each of these techniques are visible in Figs. S13 – S19. We present the outcome of processing with Neopsy software applied for the analysis of our array data in Figures S20 – S30.

Station HEI102

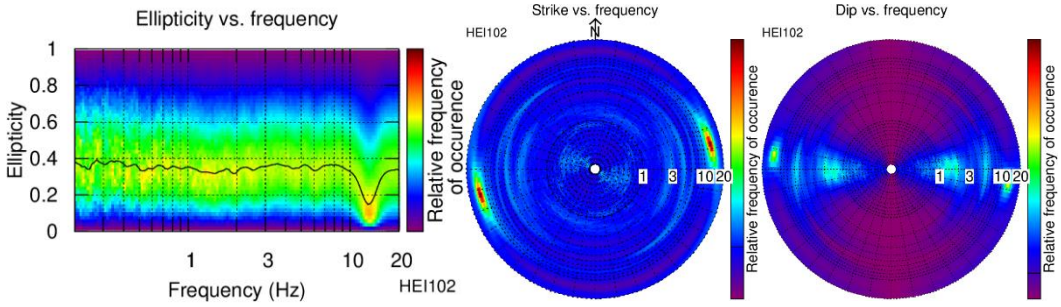

Station HEI103

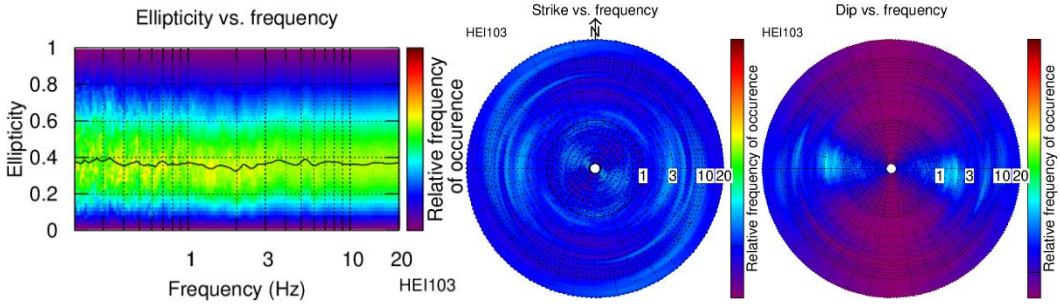

Station HEI106

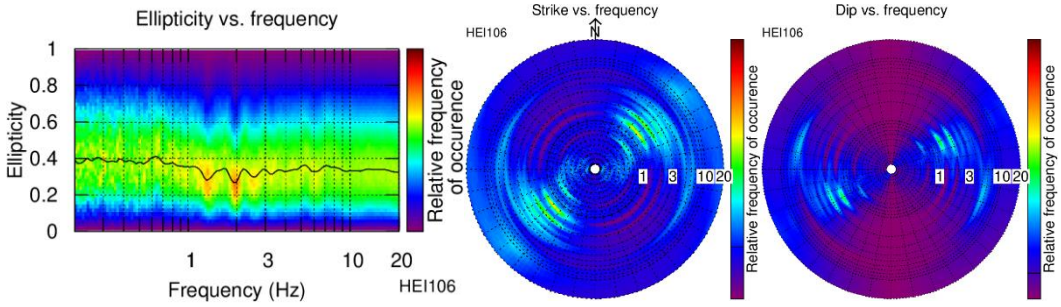

Station HEI107

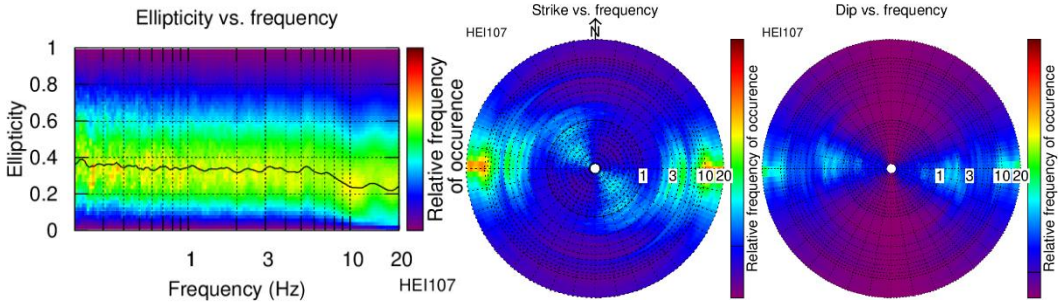

Station HEI108

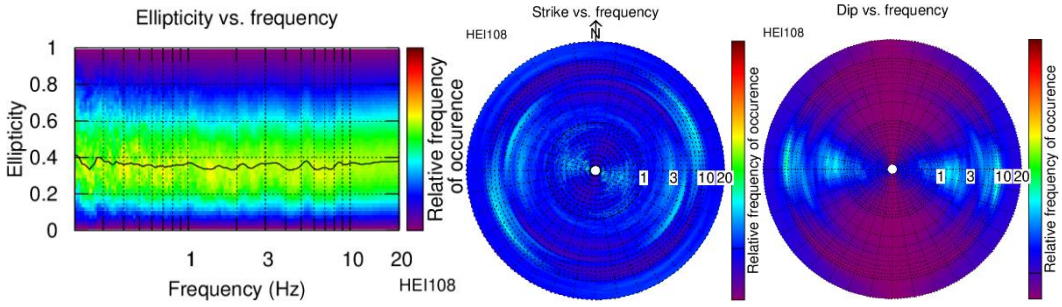

Station HEI109

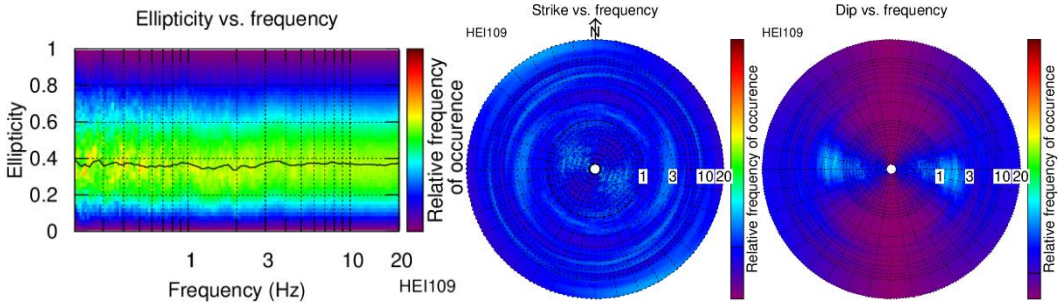

Station HEI111

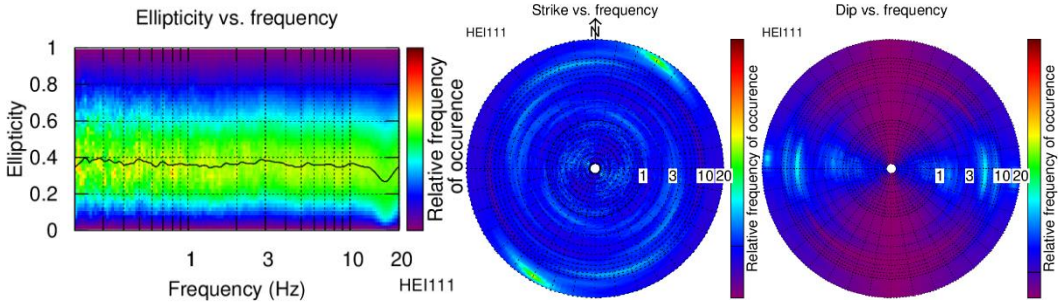

Station HEI112

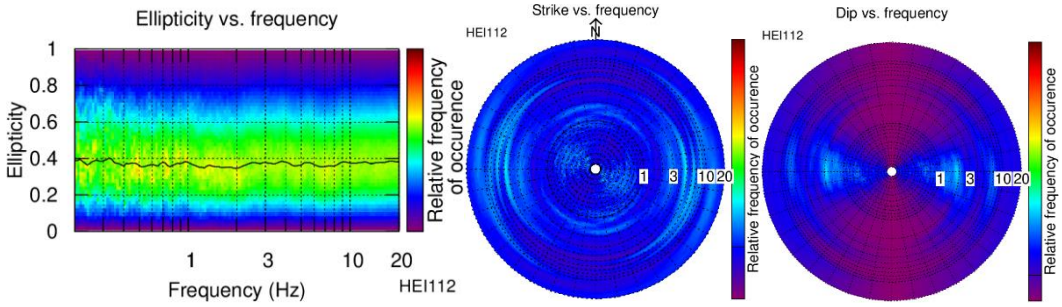

Station HEI113

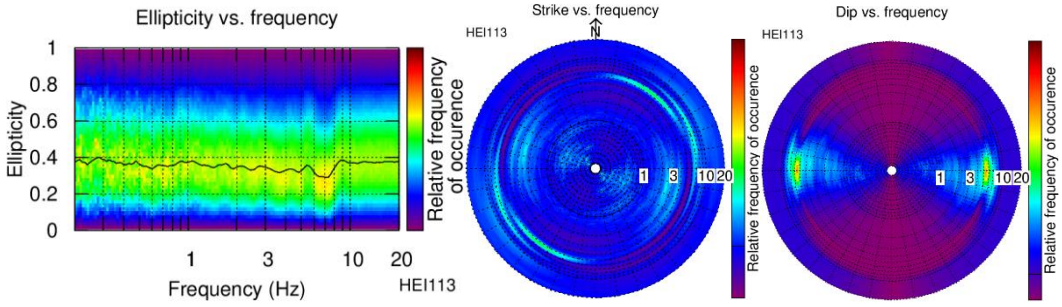

Station HEI114

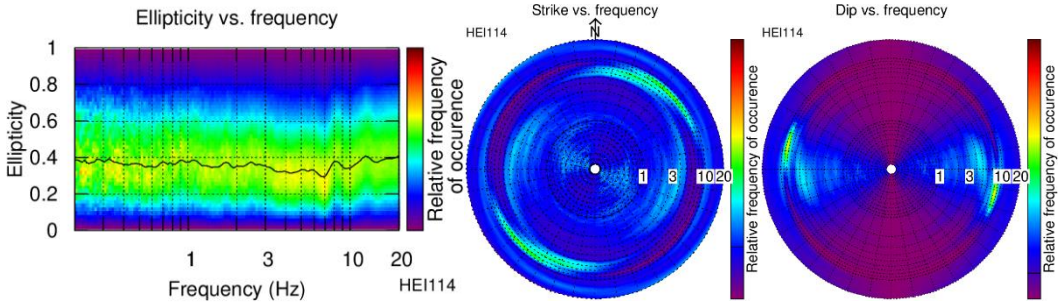

Station HEI115

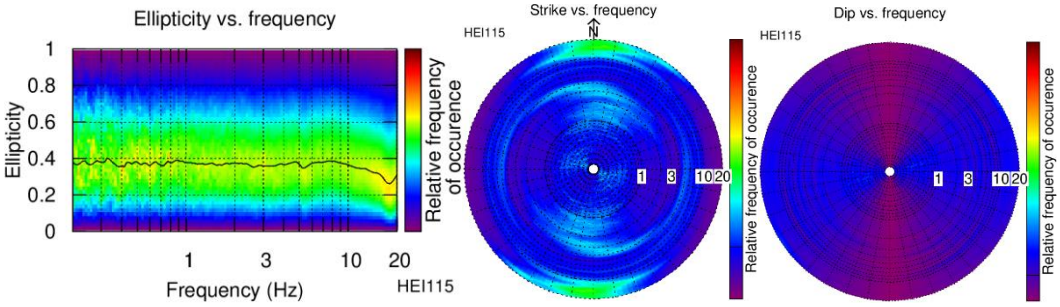

Figure S1. Results of the polarization analysis for every station of array HEI100: Particle motion ellipticity, Dip, and Strike.

Station HEI201

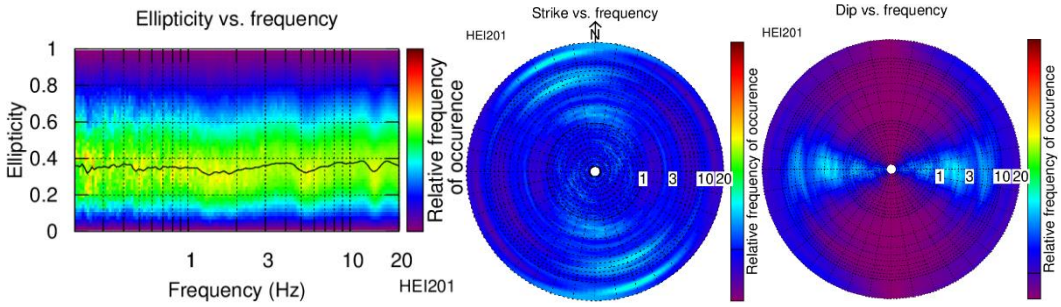

Station HEI204

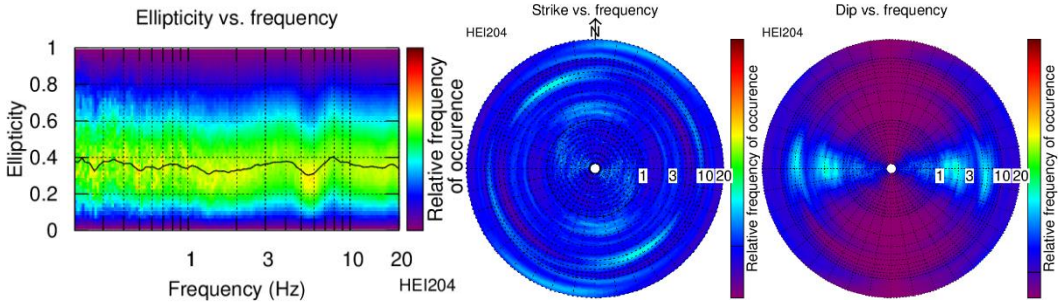

Station HEI205

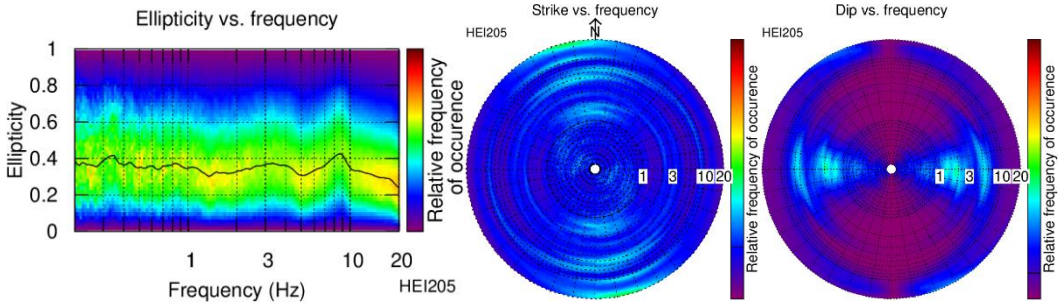

Station HEI206

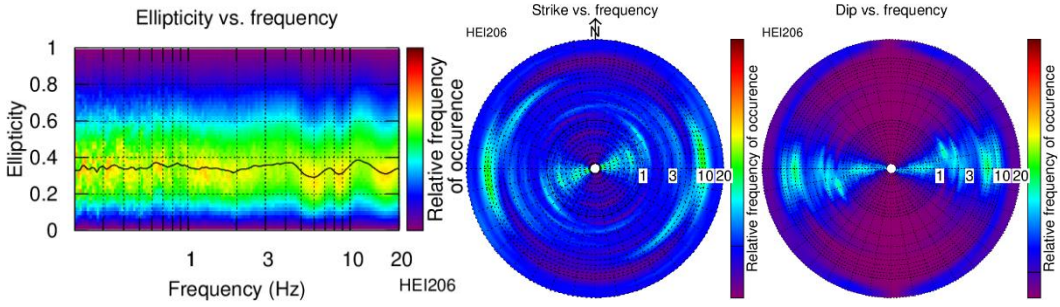

Station HEI207

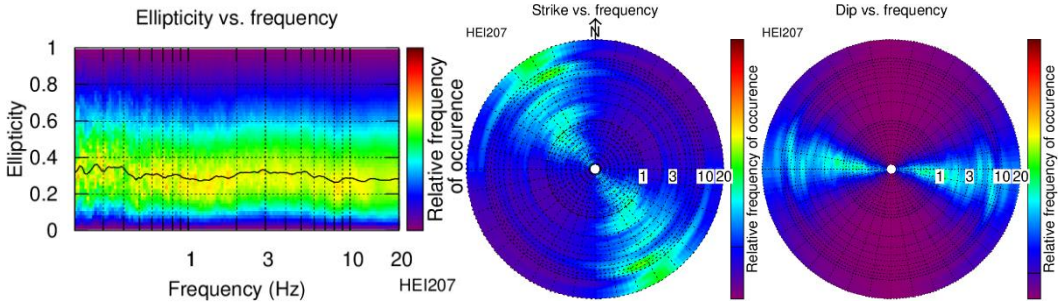

Station HEI208

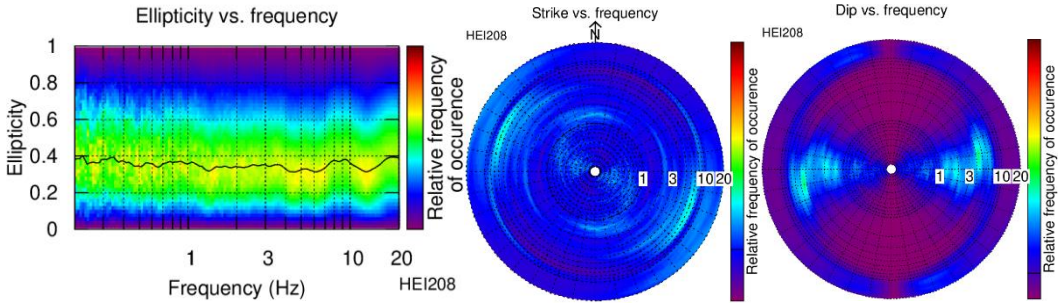

Station HEI209

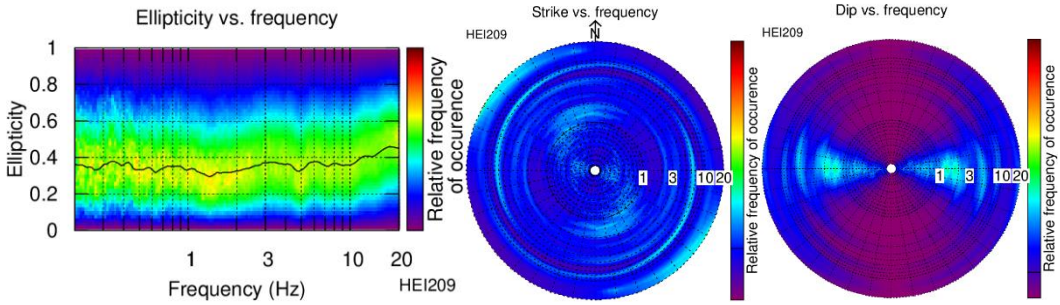

Station HEI211

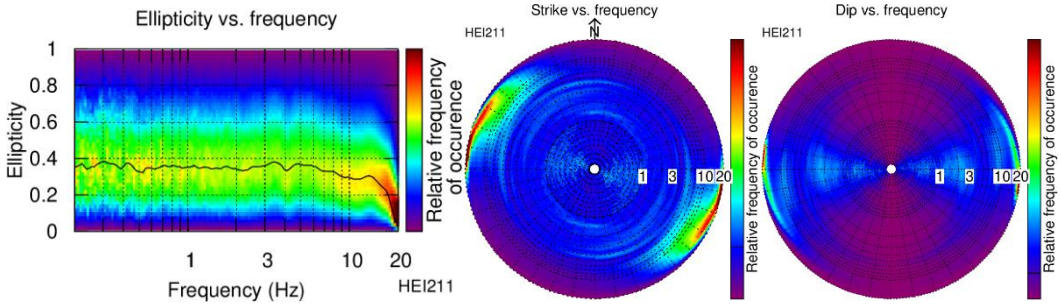

Station HEI212

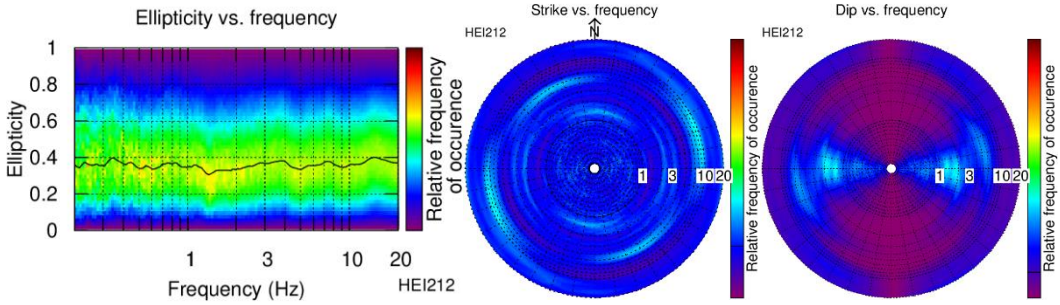

Station HEI213

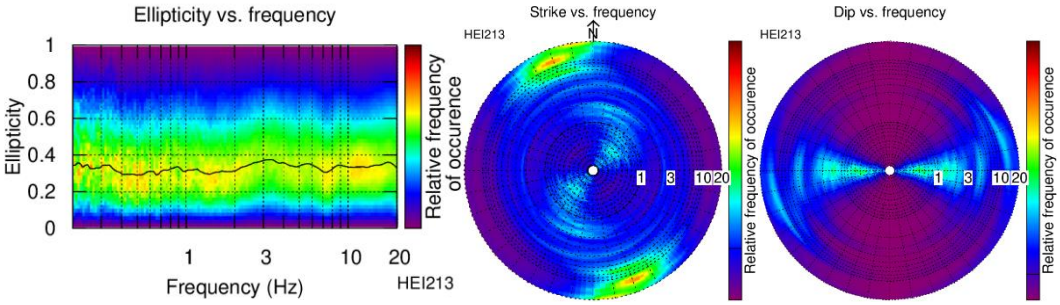

Station HEI215

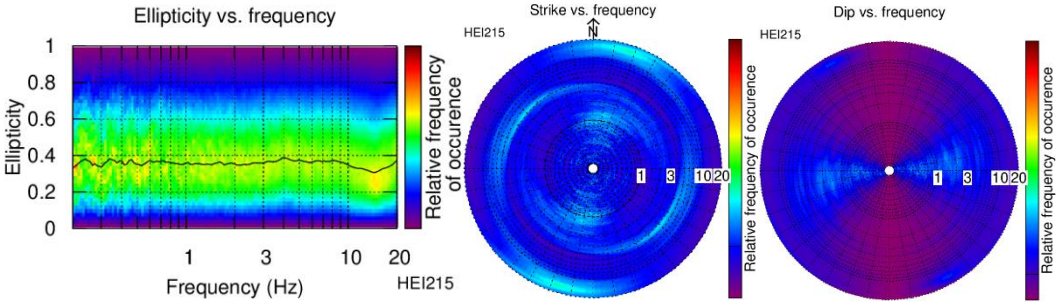

Figure S2. Results of the polarization analysis for every station of array HEI200: Particle motion ellipticity, Dip, and Strike.

Station HEI300

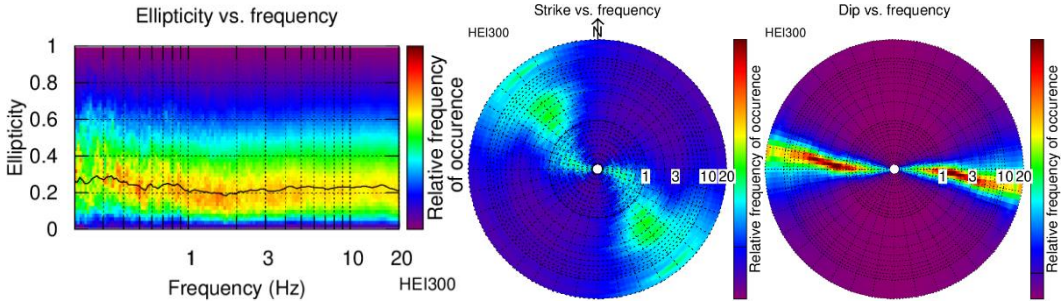

Station HEI302

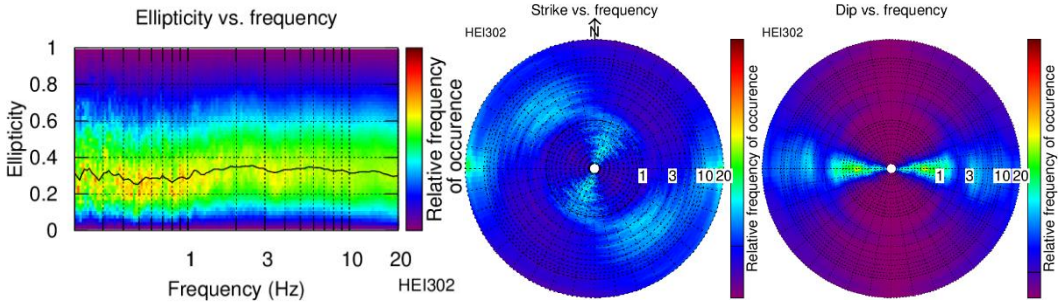

Station HEI304

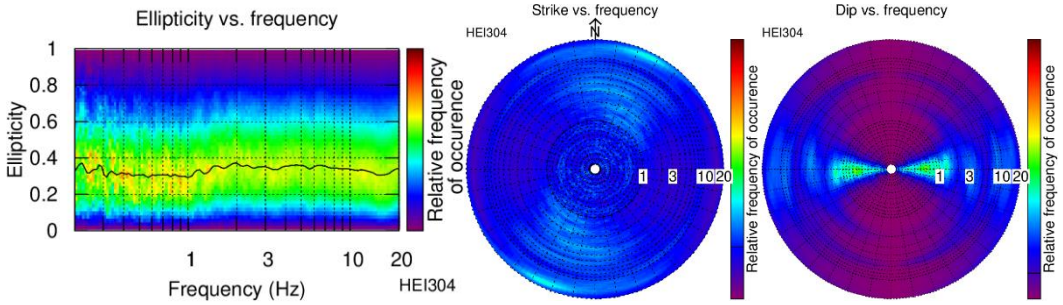

Station HEI306

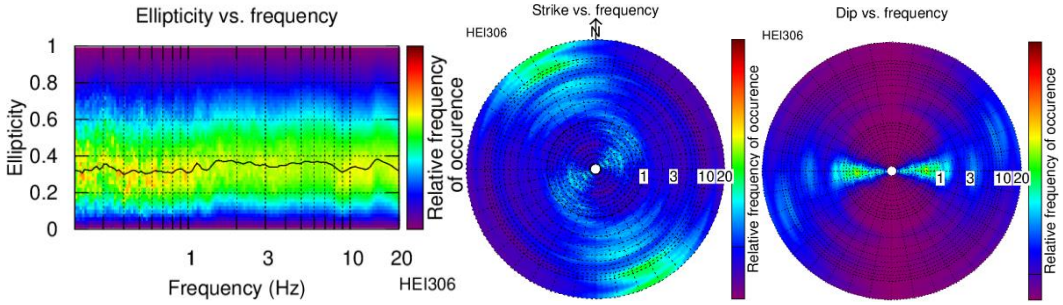

Station HEI307

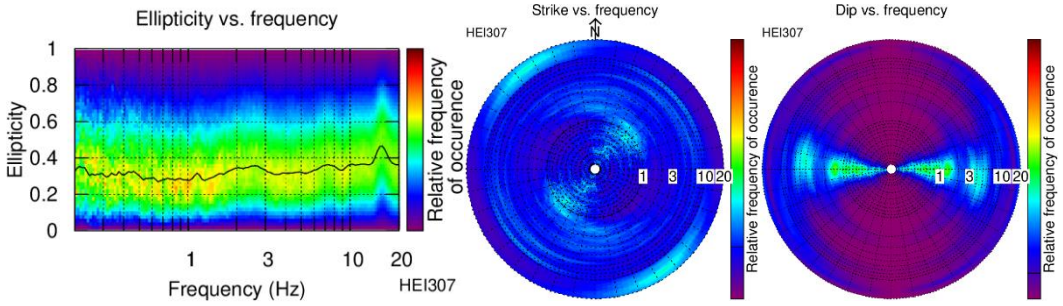

Station HEI308

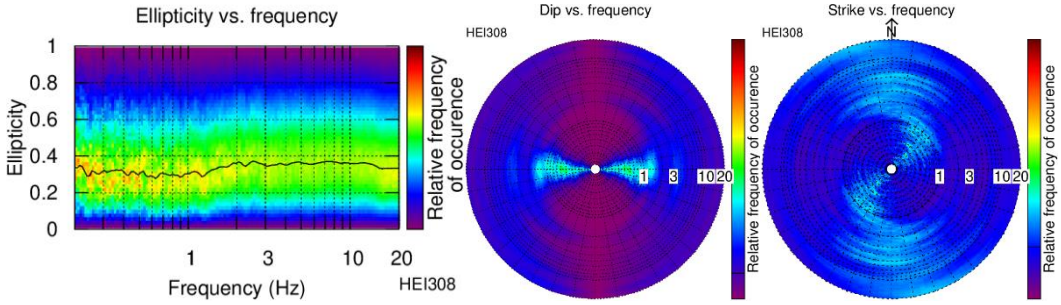

Station HEI309

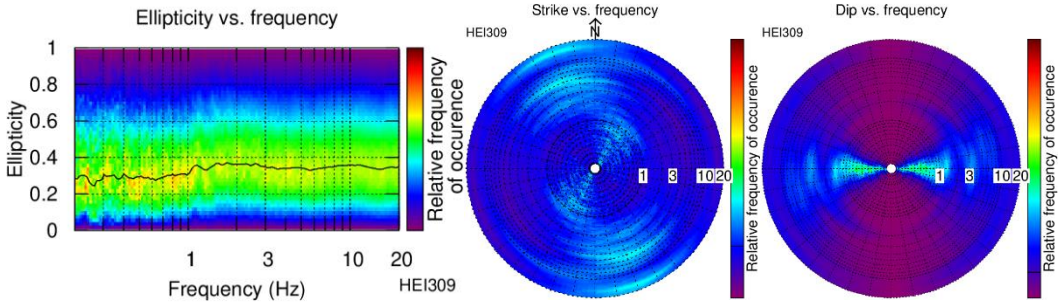

Station HEI310

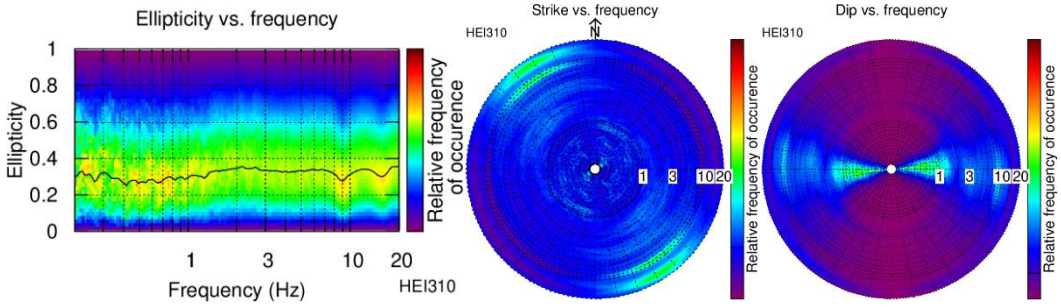

Station HEI311

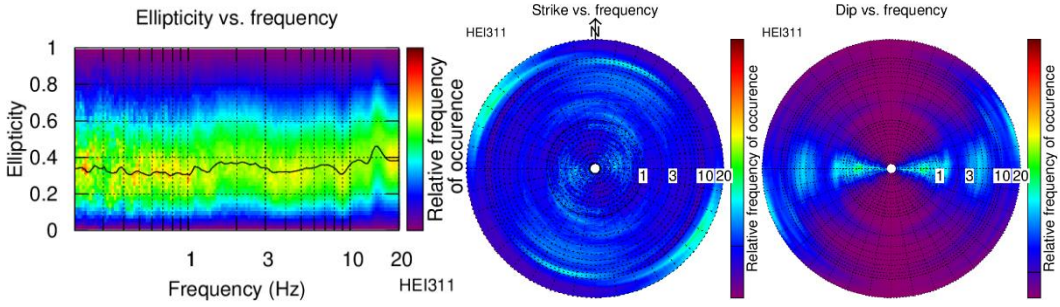

Station HEI312

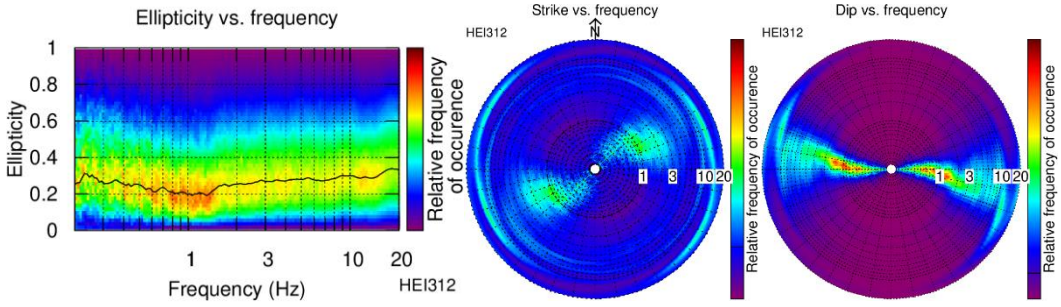

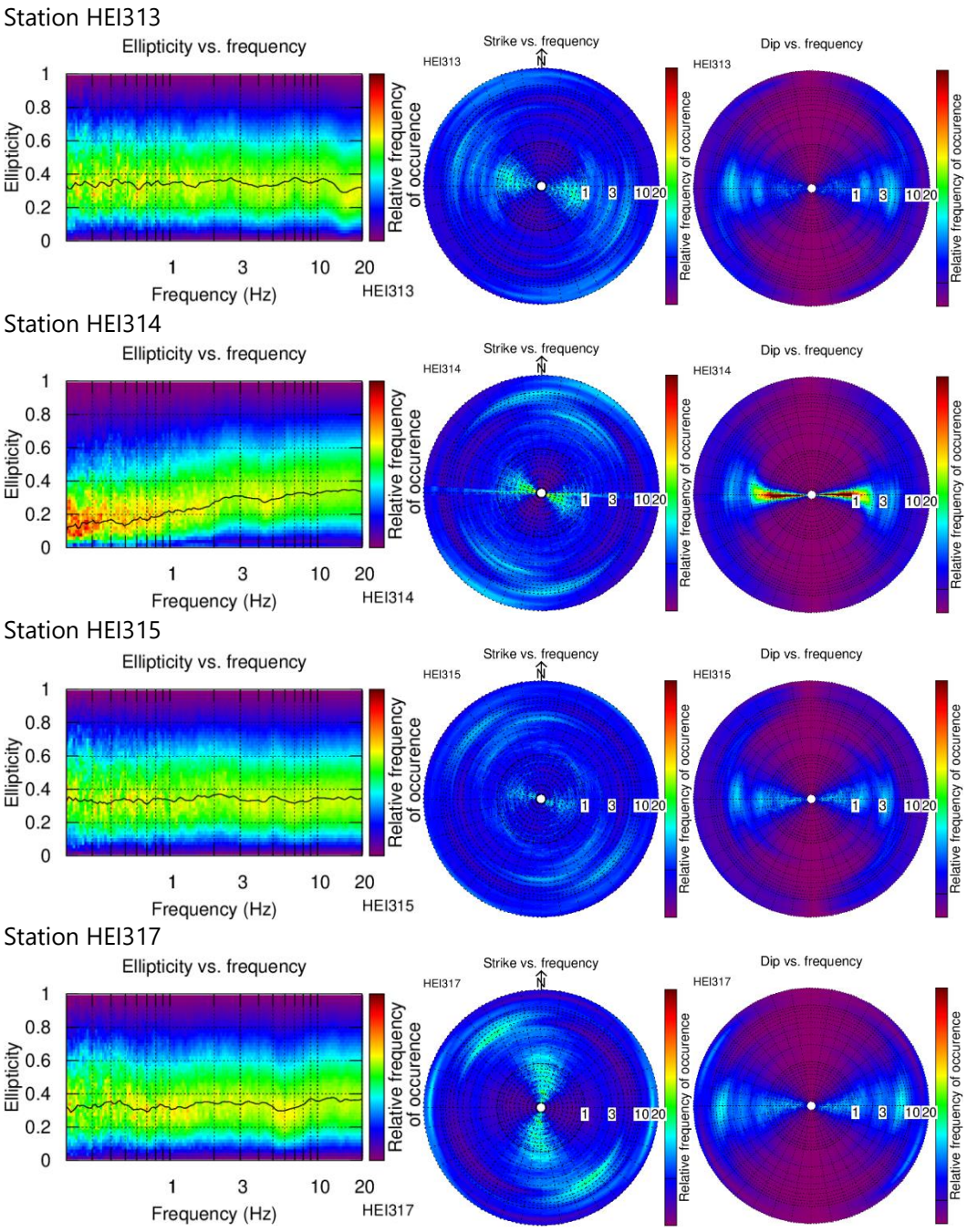

Figure S3. Results of the polarization analysis for every station of array HEI300: Particle motion ellipticity, Dip, and Strike.

Station HEI401

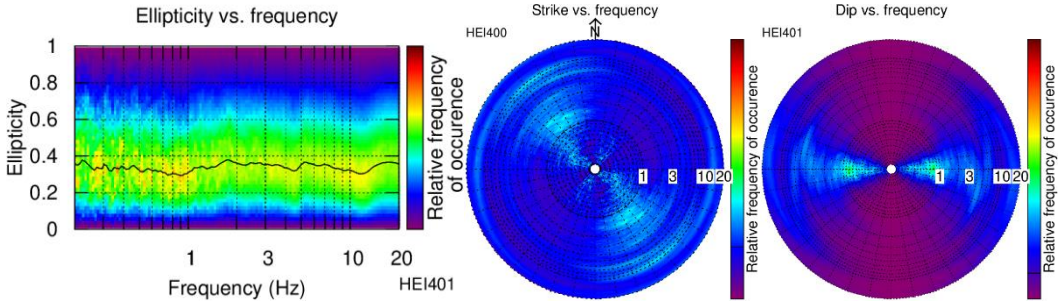

Station HEI402

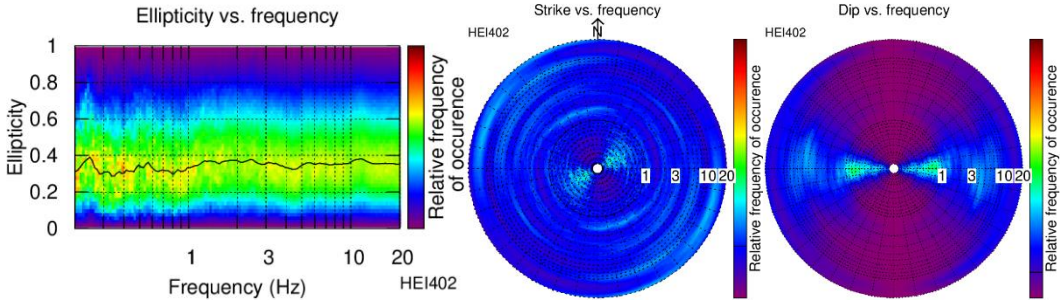

Station HEI403

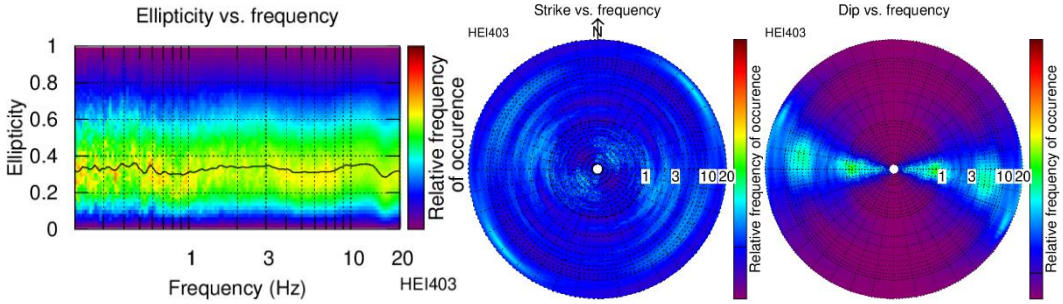

Station HEI404

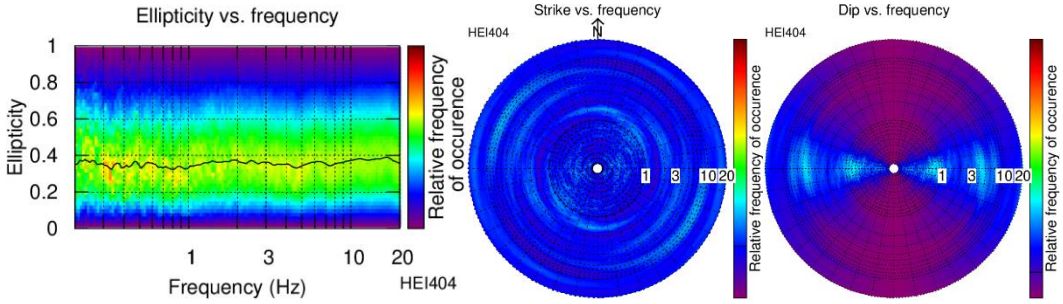

Station HEI406

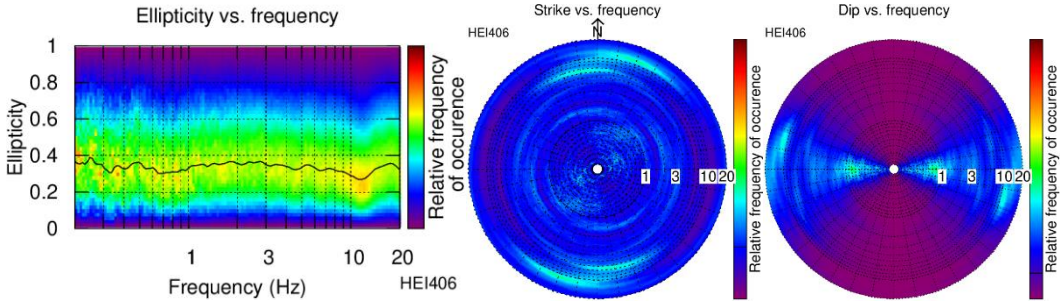

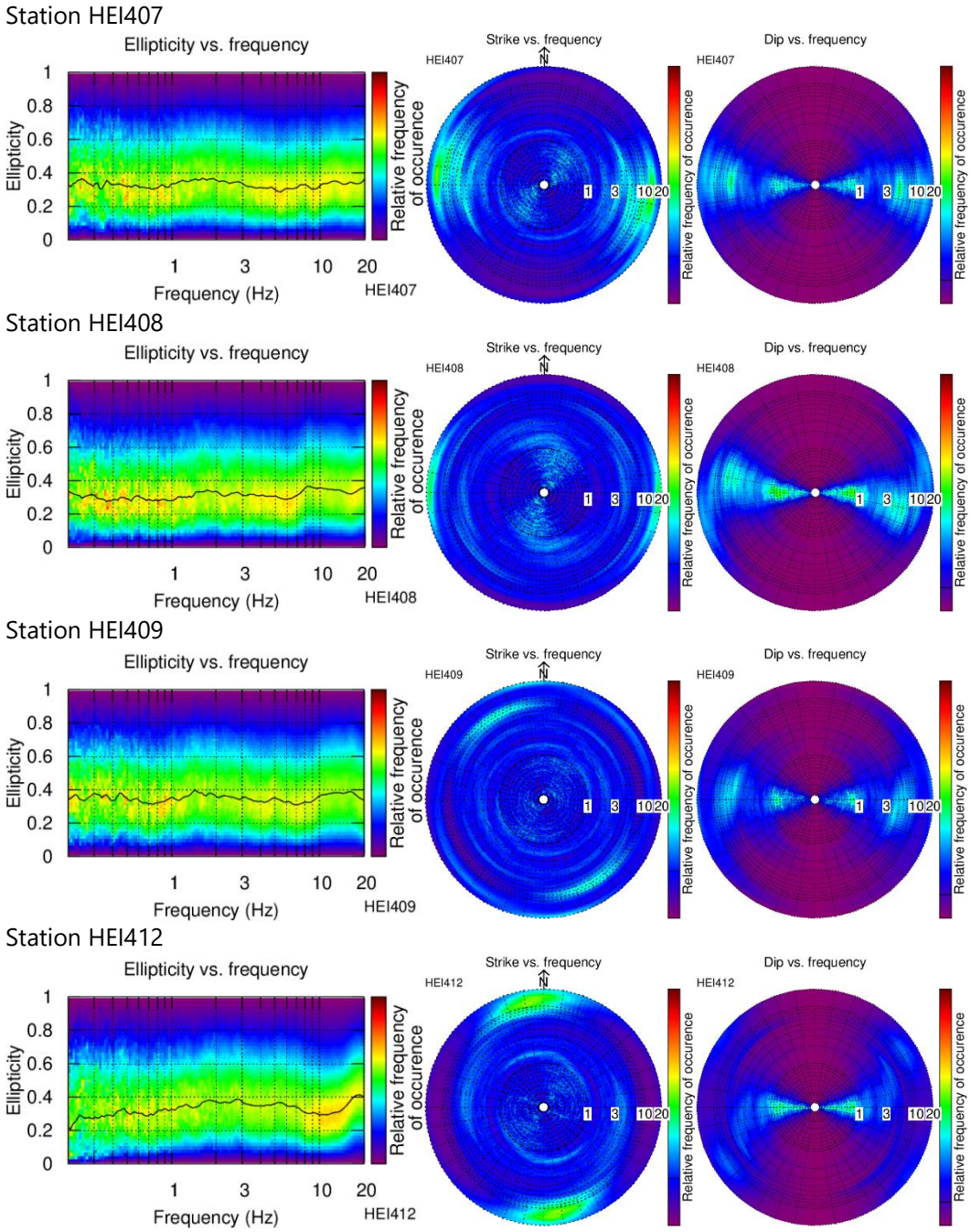

Figure S4. Results of the polarization analysis for every station of array HEI400: Particle motion ellipticity, Dip, and Strike.

Station HEI500

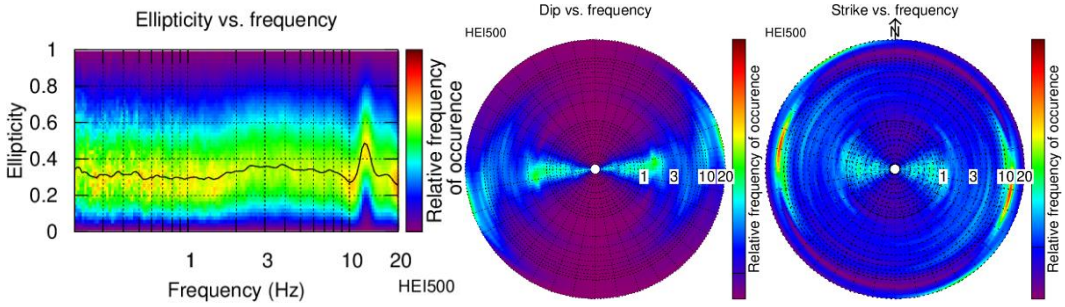

Station HEI501

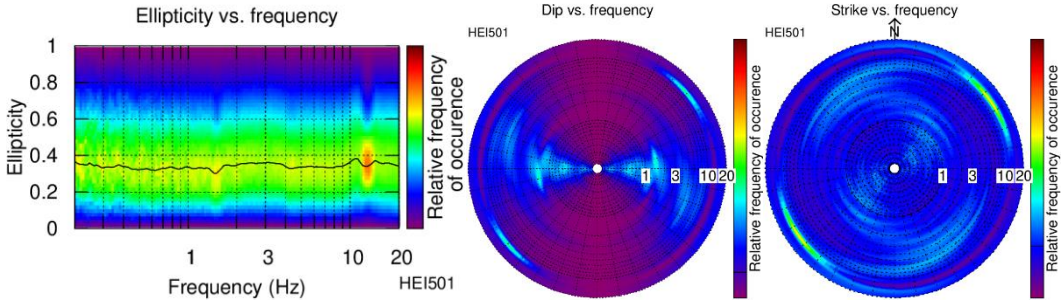

Station HEI503

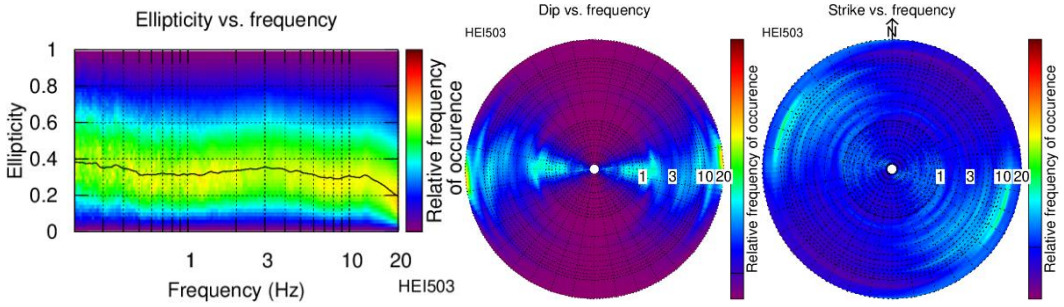

Station 504

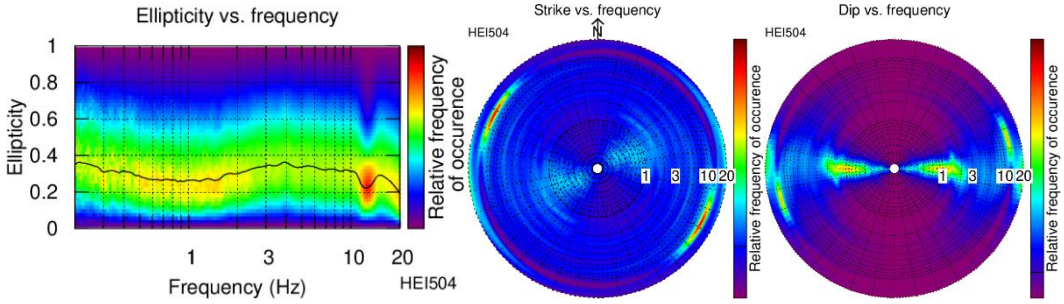

Station HEI506

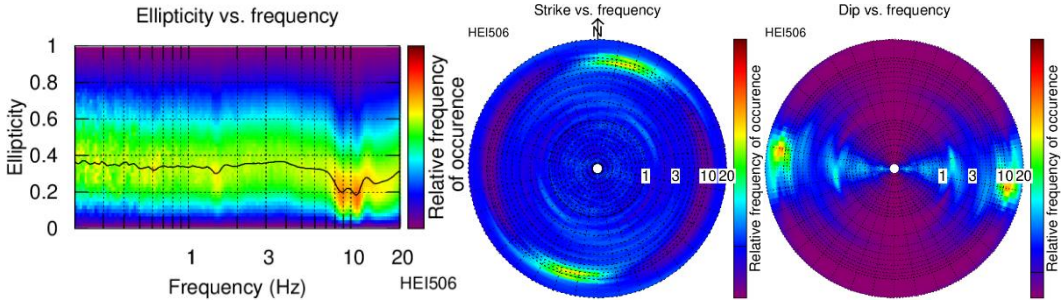

Station HEI507

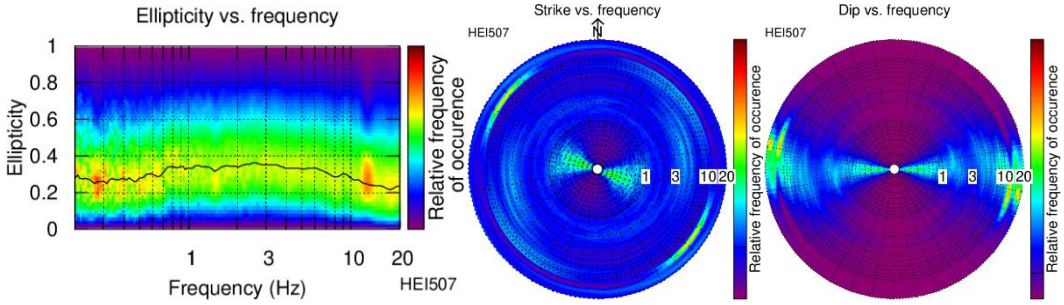

Station HEI508

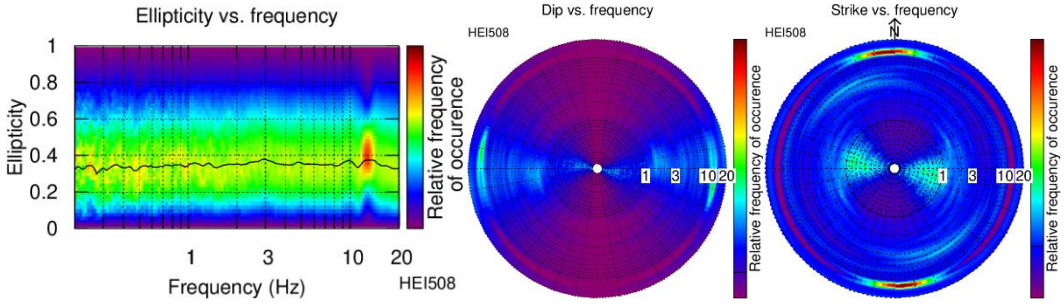

Station HEI509

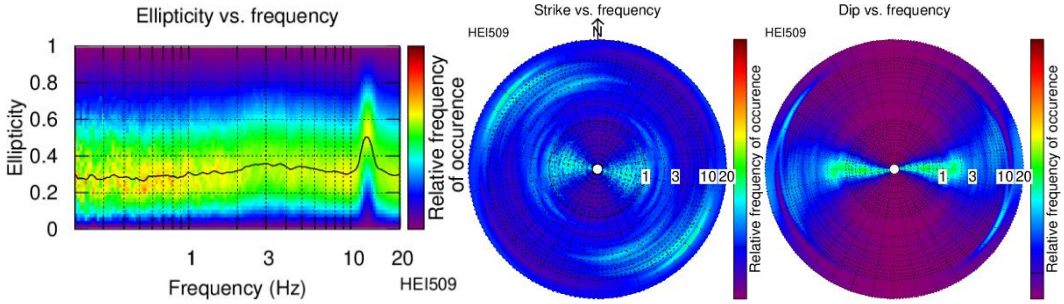

Station 510

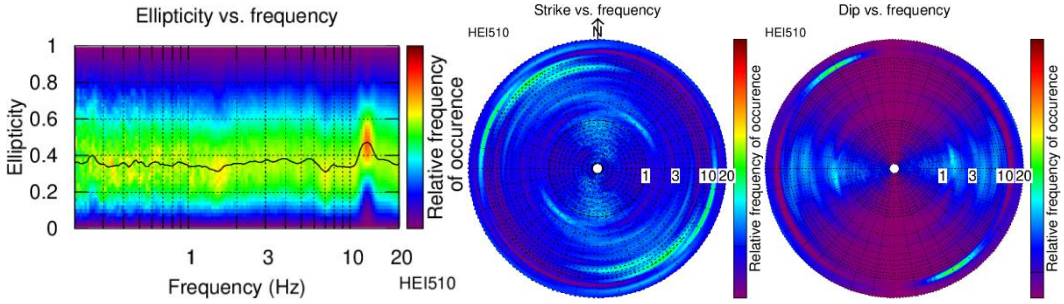

Station 511

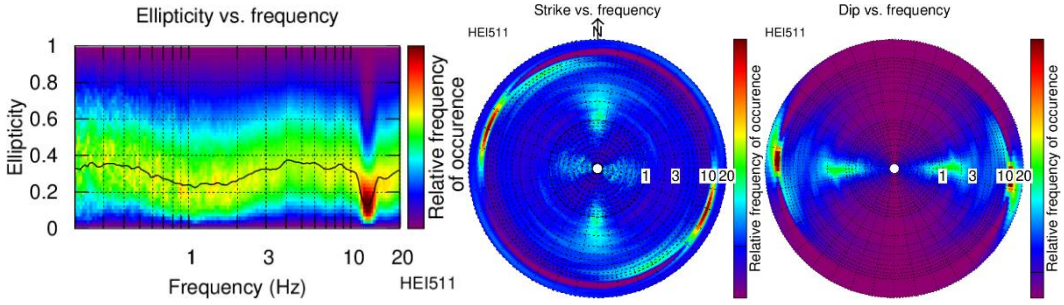

Station 512

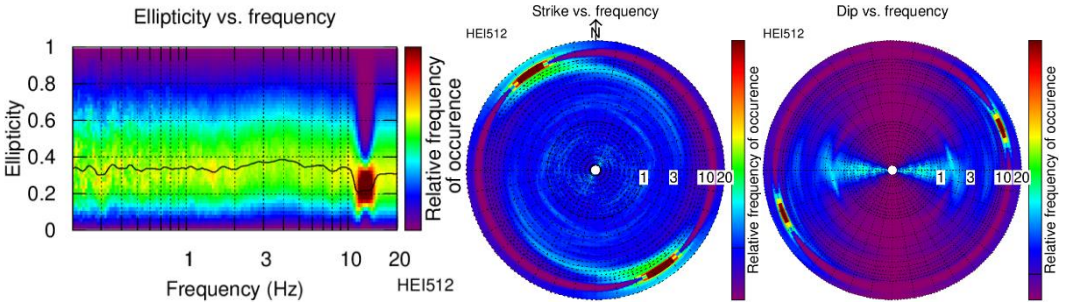

Figure S5. Results of the polarization analysis for every station of array HEI500: Particle motion ellipticity, Dip, and Strike.

HEI100

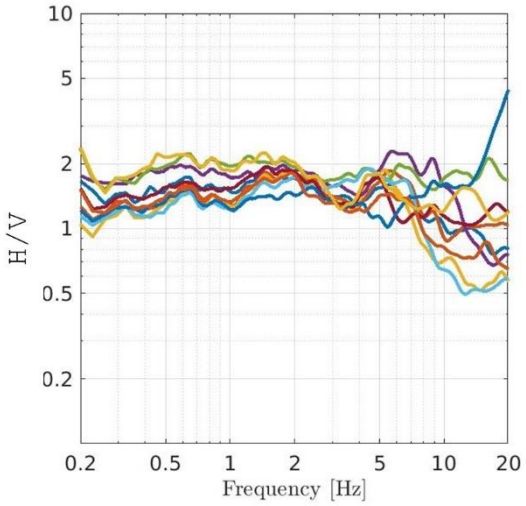

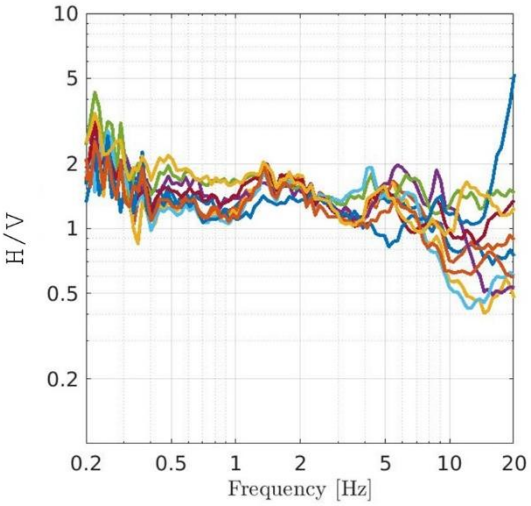

HEI200

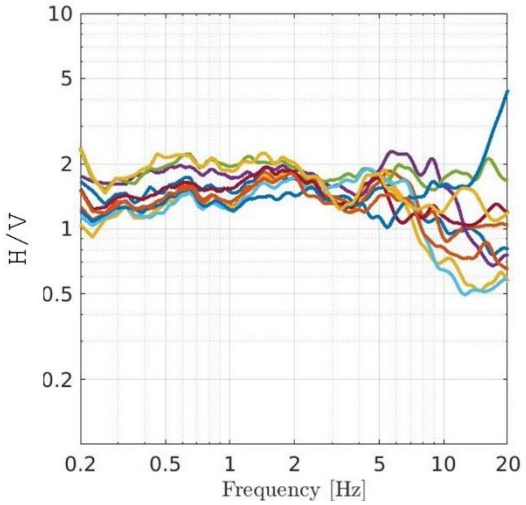

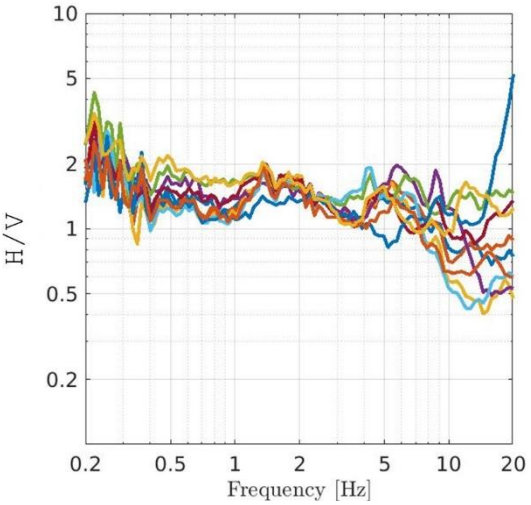

HEI300

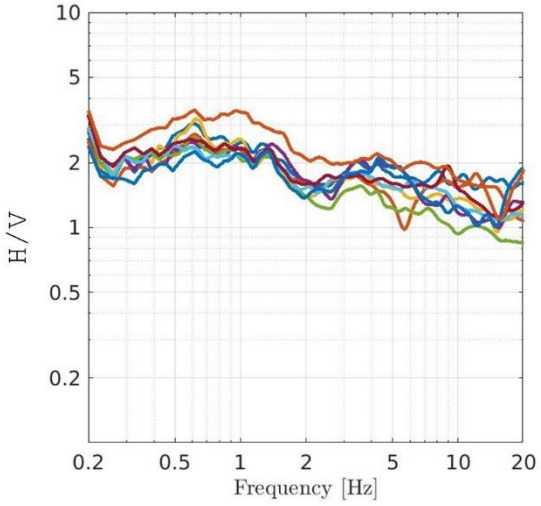

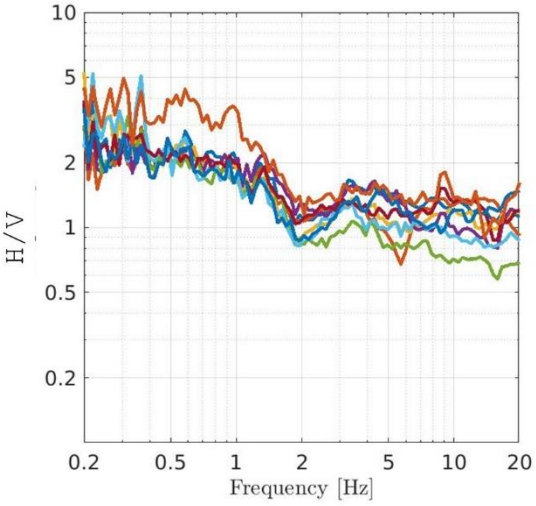

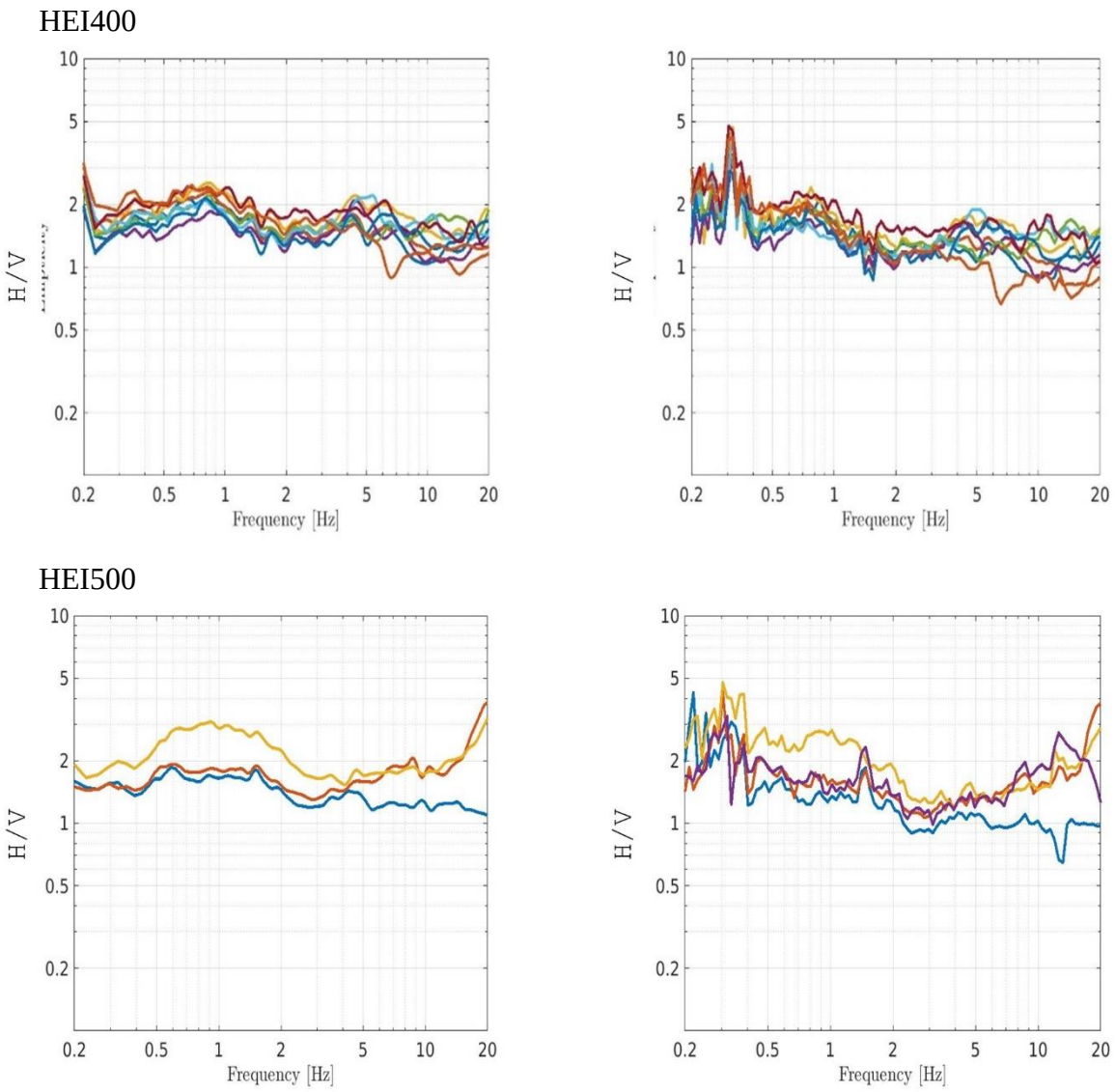

Figure S6. The H/V curves for selected stations of the presented arrays in classic (left) and raydec (right). Individual stations of the array are represented by colors.

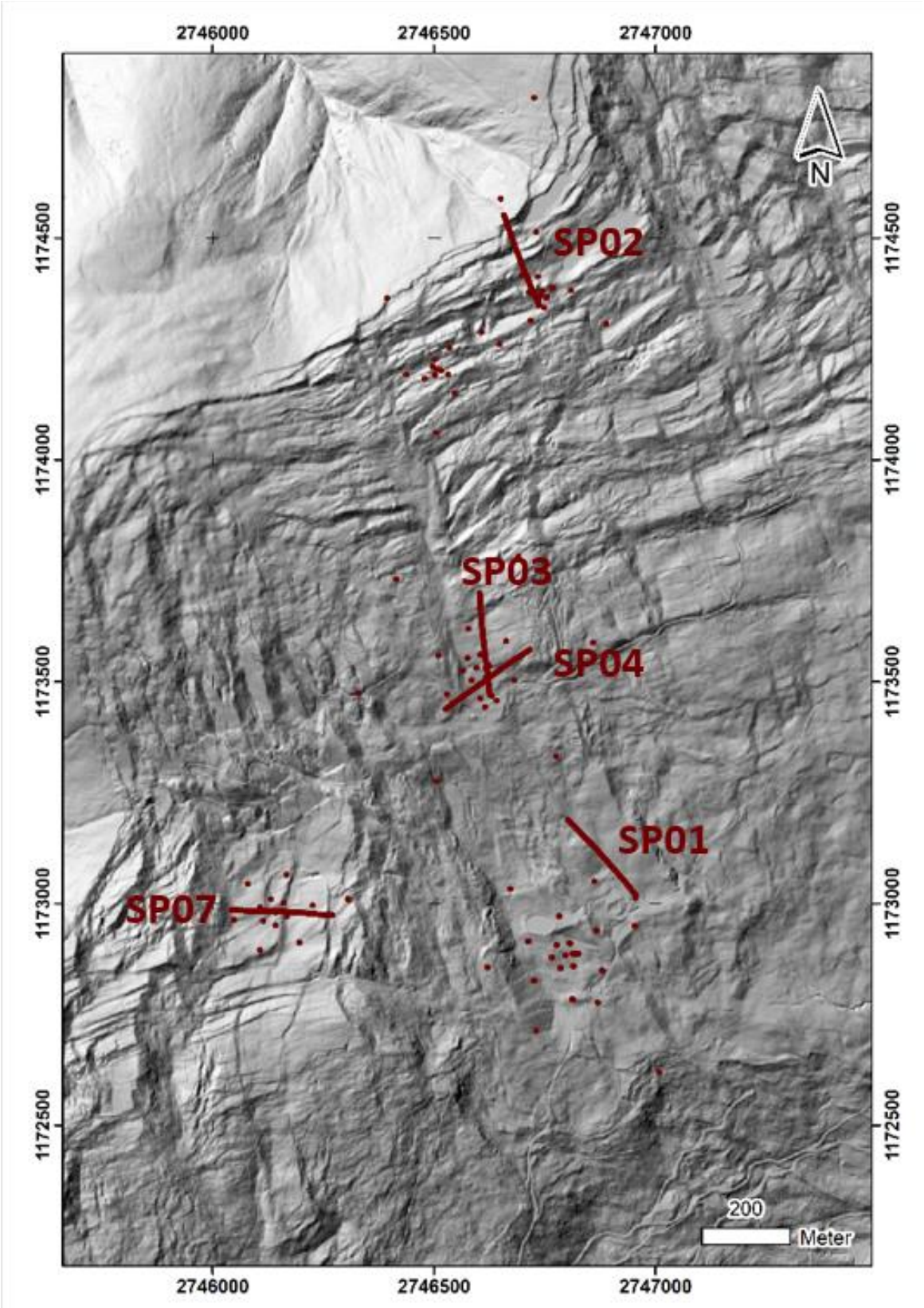

Figure S7. Map of all SRT profiles in the Heinzenberg Landslide.

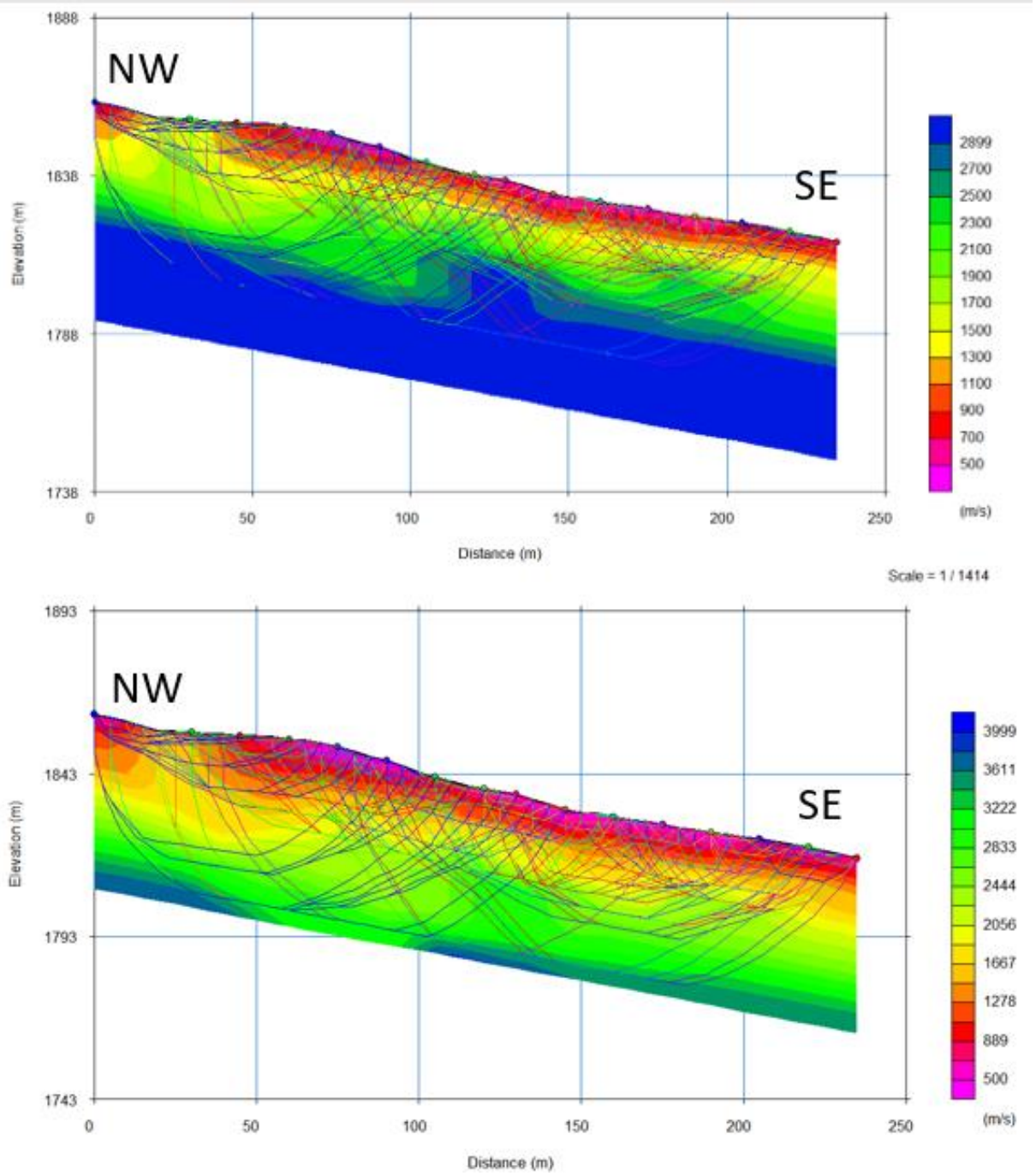

Figure S8. SP01 profile. The inferred P-wave velocity is shown by color and lines are estimated wave travel paths with two different color scales, i.e., 500-3100 m/s and 500-4200 m/s, respectively.

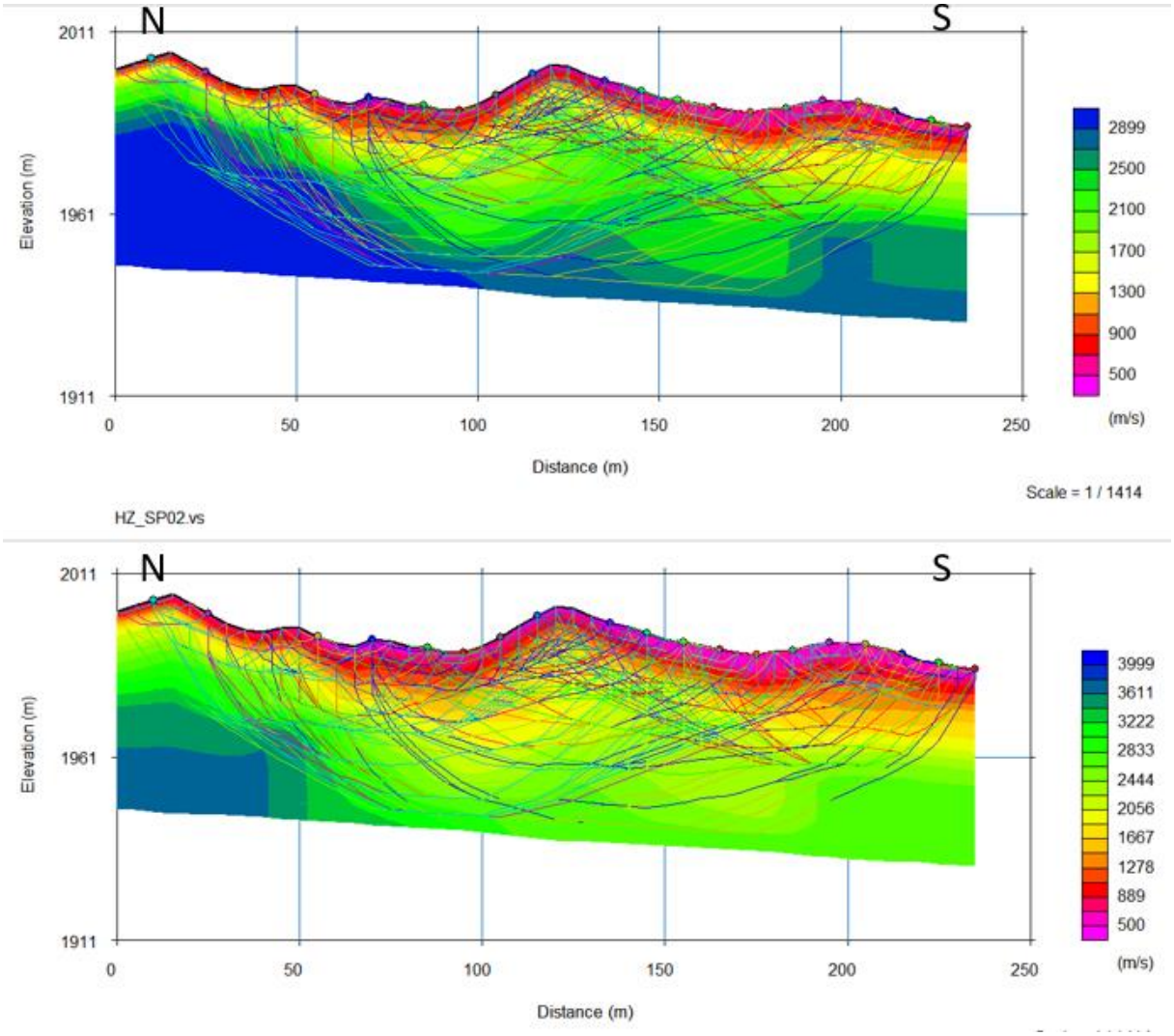

Figure S9. SP02 profile. The inferred P-wave velocity is shown by color and lines are estimated wave travel paths with two different color scales, i.e., 500-3100 m/s and 500-4200 m/s, respectively.

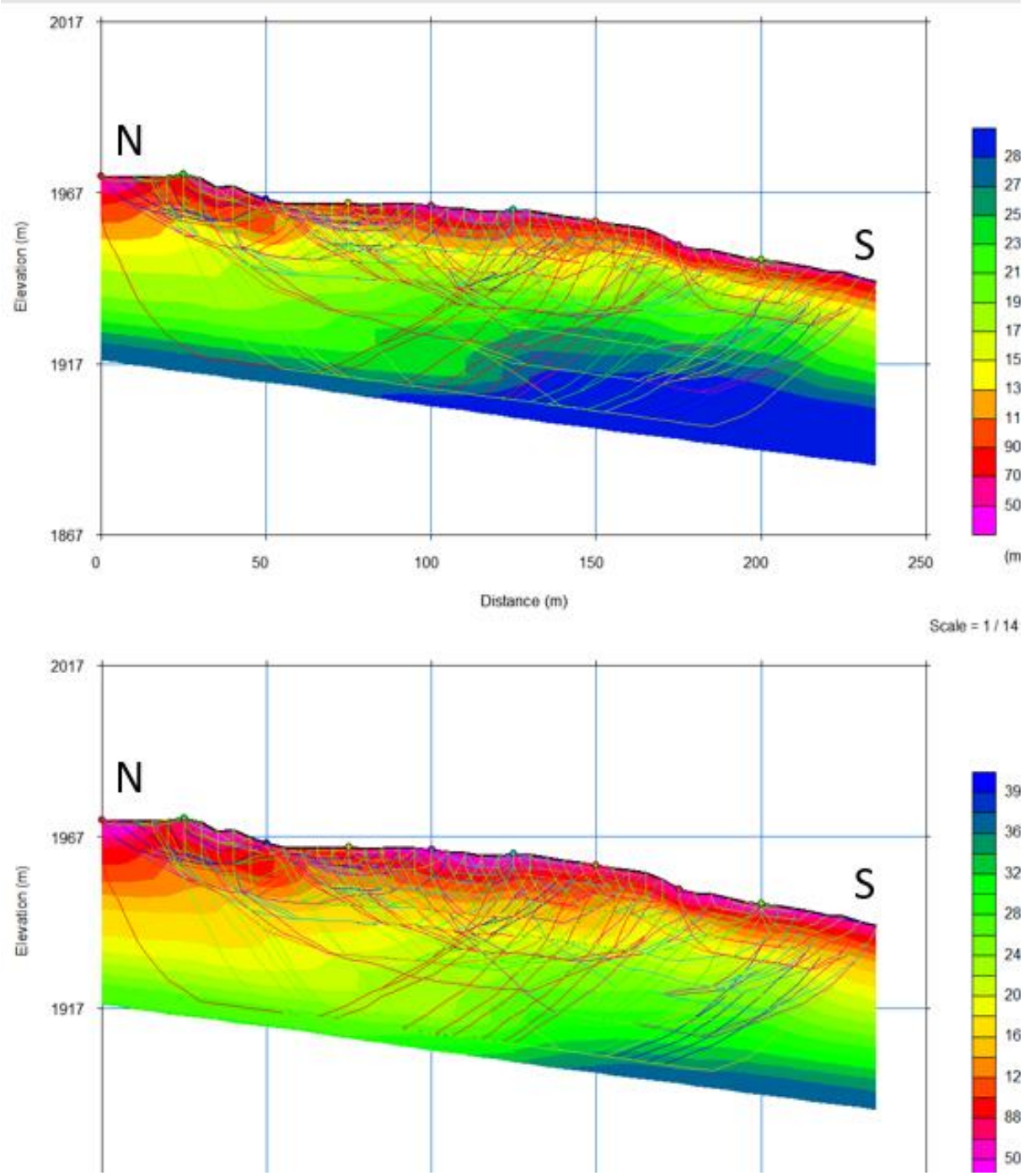

Figure S10. SP03 profile. The inferred P-wave velocity is shown by color and lines are estimated wave travel paths with two different color scales, i.e., 500-3100 m/s and 500-4200 m/s, respectively.

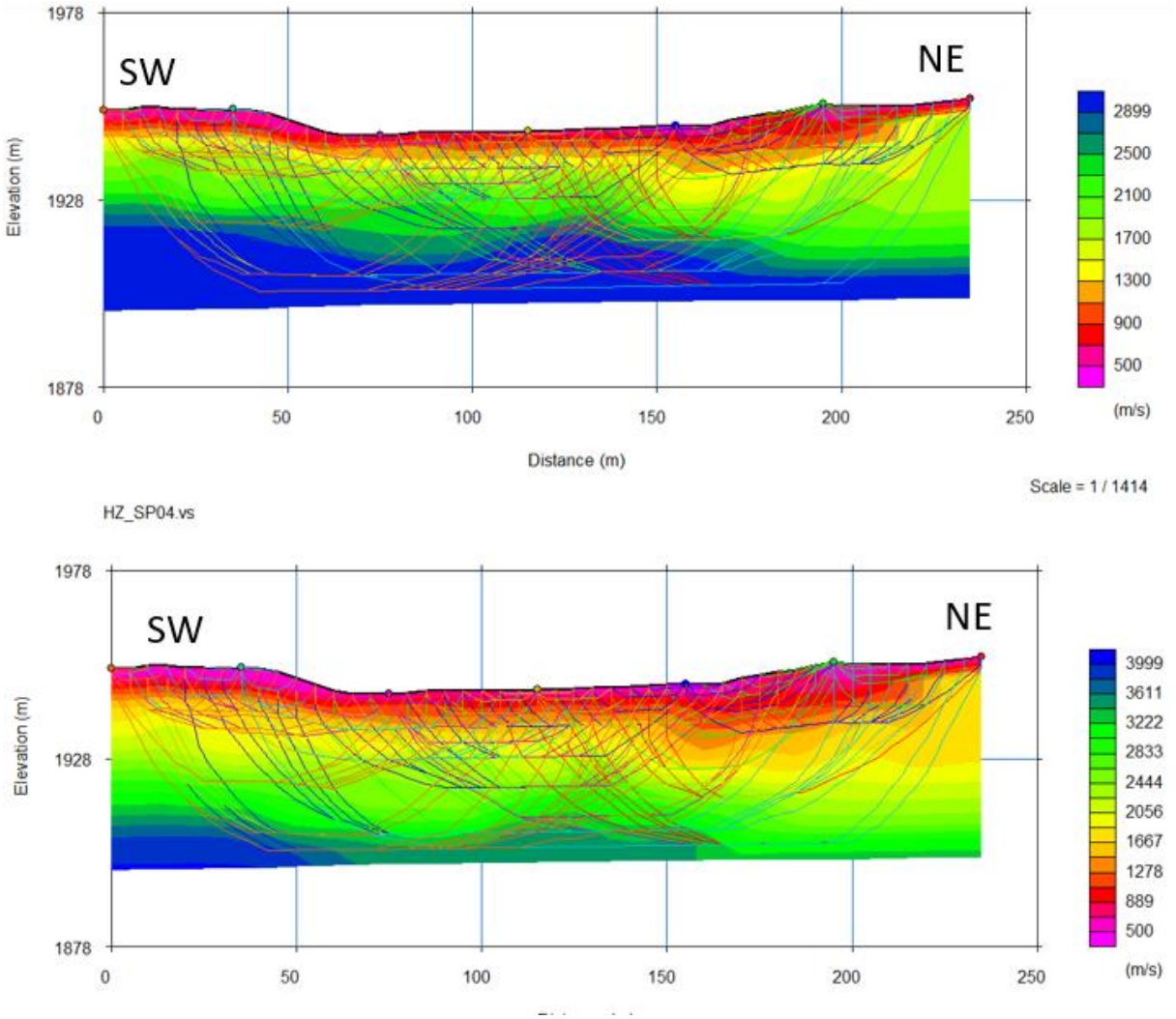

Figure S11. SP04 profile. The inferred P-wave velocity is shown by color and lines are estimated wave travel paths with two different color scales, i.e., 500-3100 m/s and 500-4200 m/s, respectively.

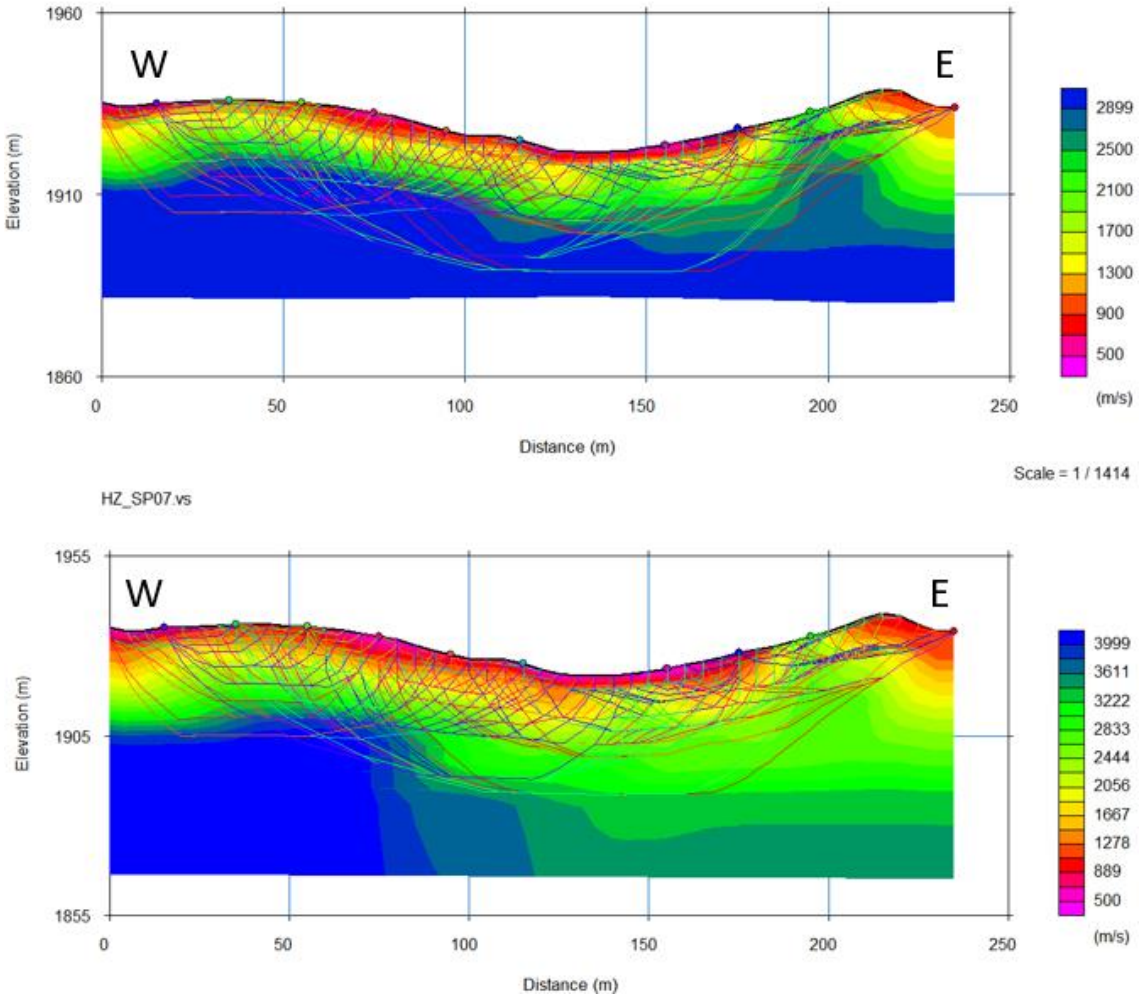

Figure S12. SP07 profile. The inferred P-wave velocity is shown by color and lines are estimated wave travel paths with two different color scales, i.e., 500-3100 m/s and 500-4200 m/s, respectively**.**

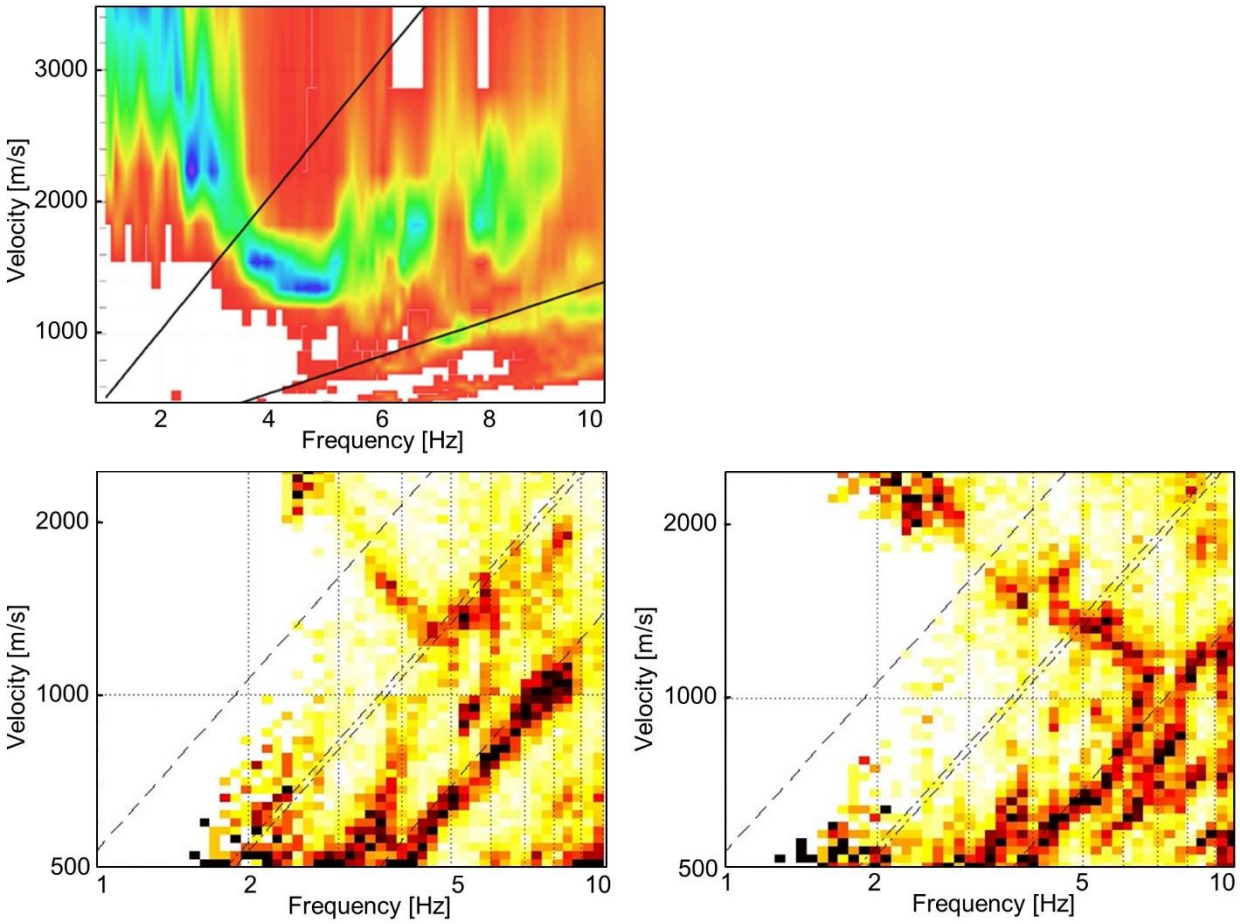

Figure S13. HEI100 velocity dispersion of all data using 1CFK (top left), vertical component (bottom left), and transversal component from 3CFK (bottom right).

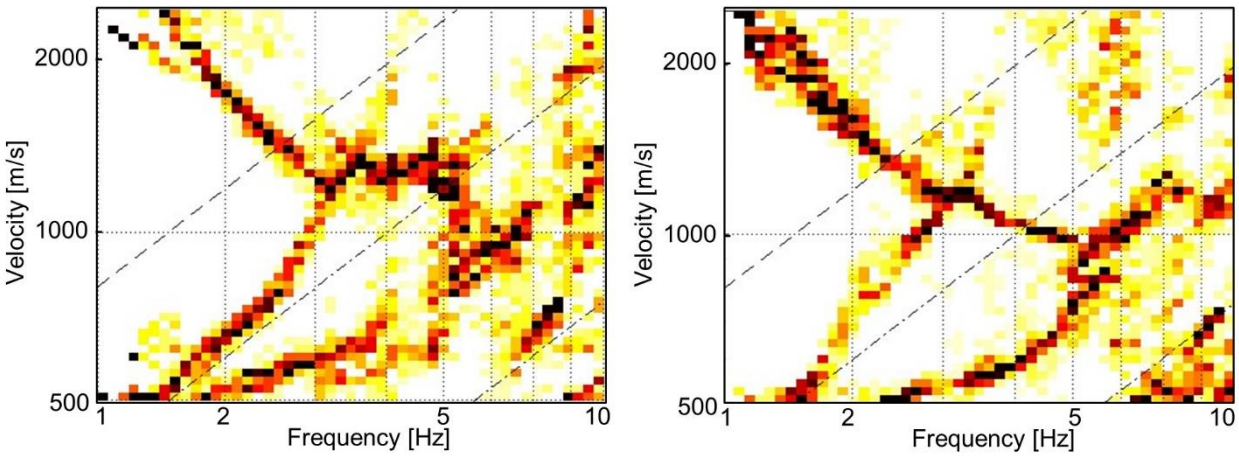

Figure S14. HEI200 velocity dispersion of vertical component (left) and transversal component (right) from 3CFK.

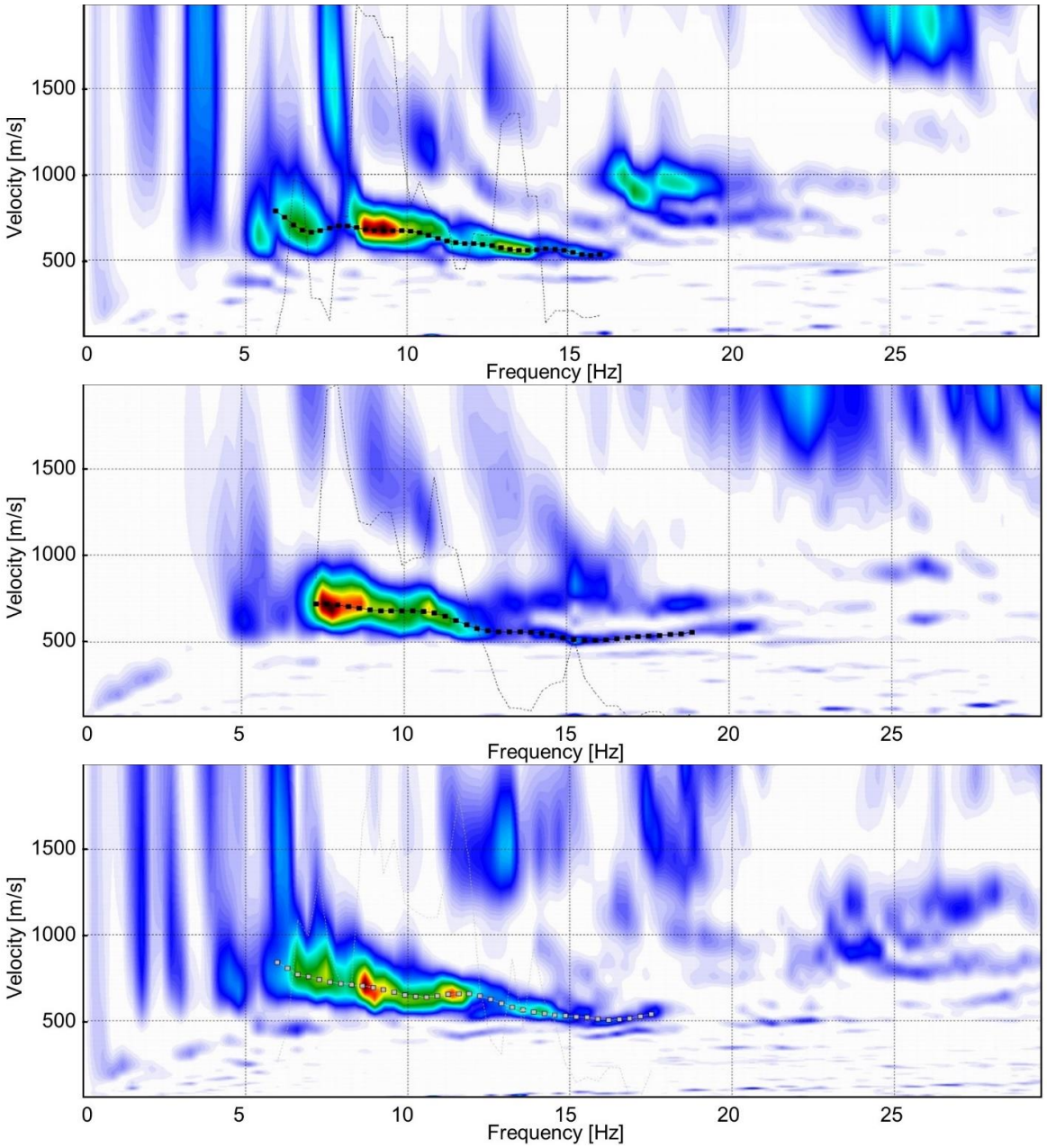

Figure S15. Dispersion curves from MASW on profiles SP03N (top), SP03S (middle) and SP04SW (bottom).

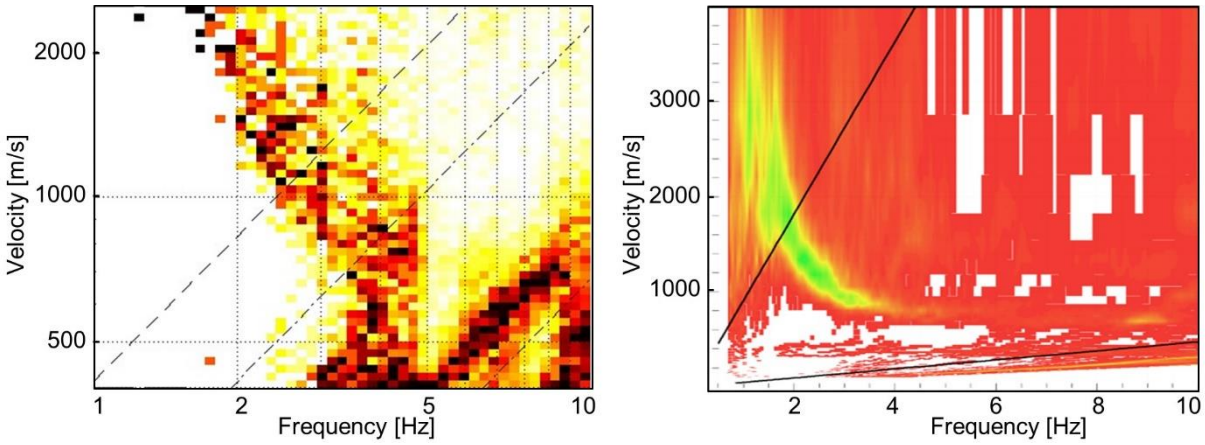

Figure S16. HEI300 velocity dispersion from 1CFK (left) and vertical component from 3CFK (right).

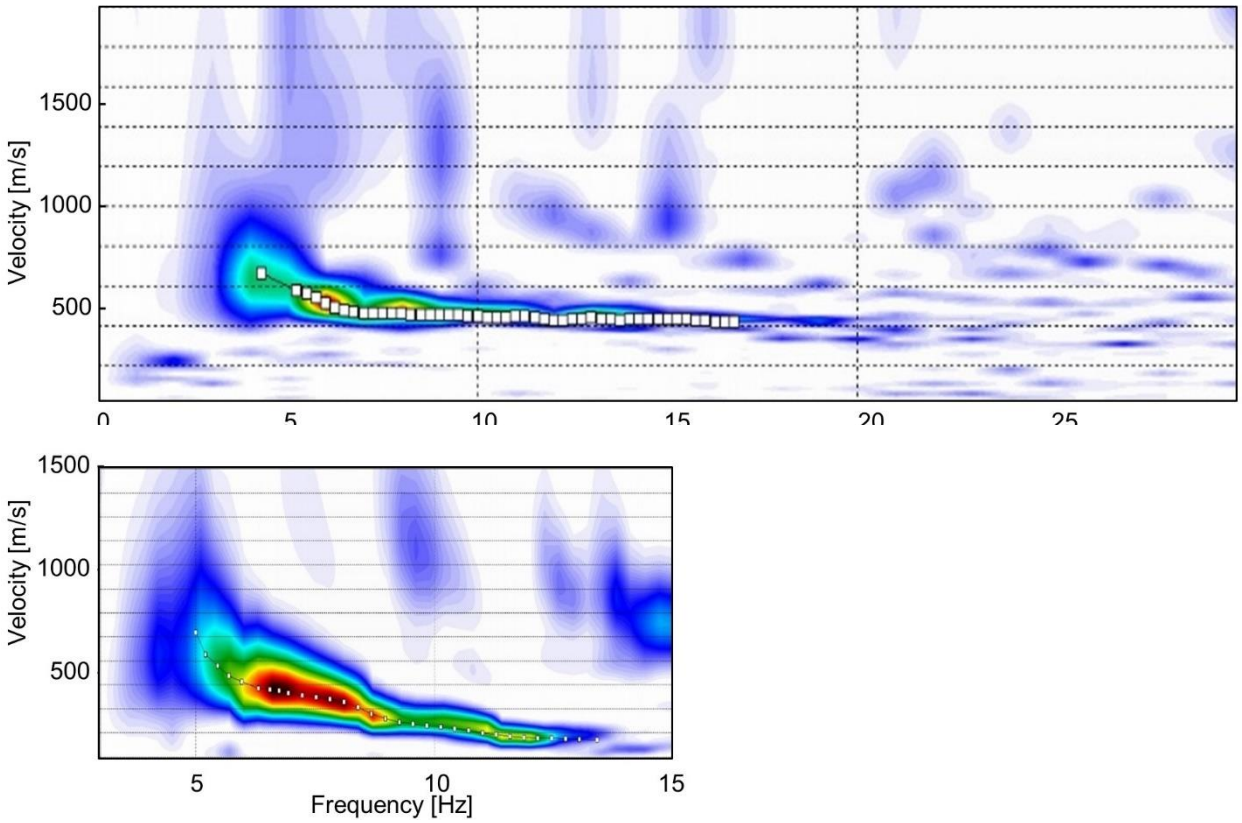

Figure S17. Dispersion curves from MASW along the profiles SP01 SE (top) and SP01 NW (bottom).

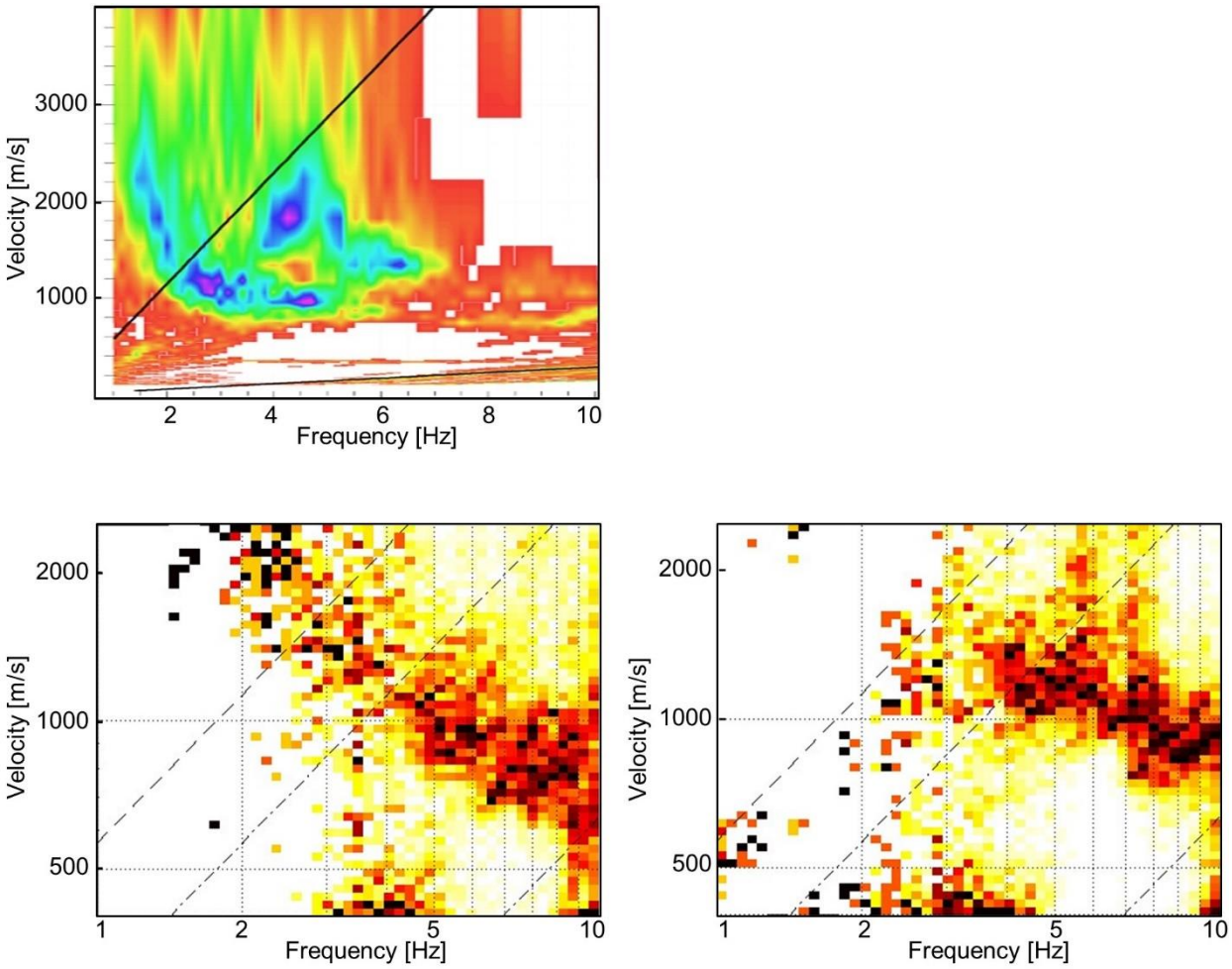

Figure S18. HEI400 velocity dispersion from 1CFK (top left), and from the inner array with 3CFK: vertical component (bottom left) and transversal component (bottom right).

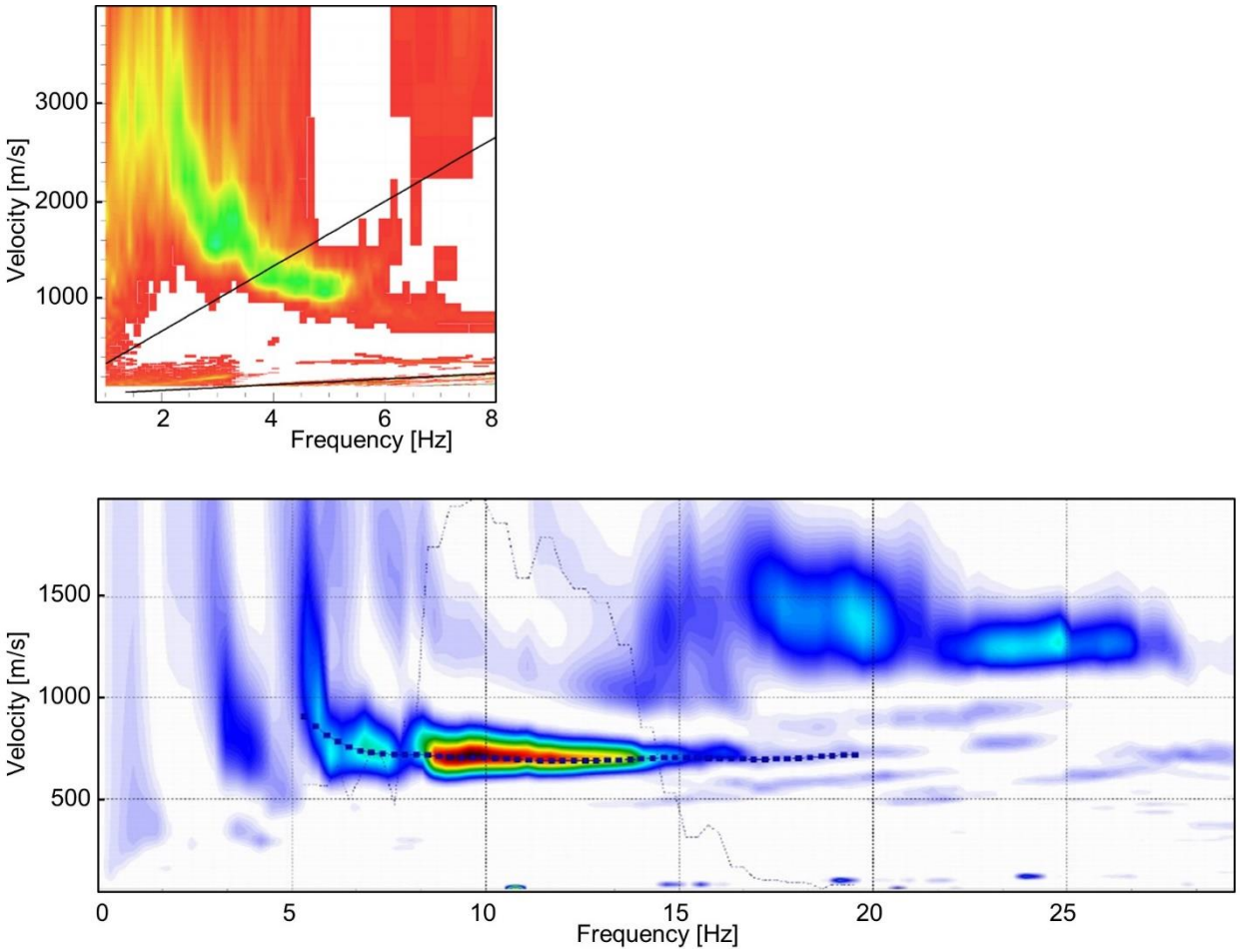

Figure S19. Rayleigh wave velocity dispersion of HEI500 from 1CFK (top left) and MASW results of SP07 from W to E (bottom).

HEI100 R0L0

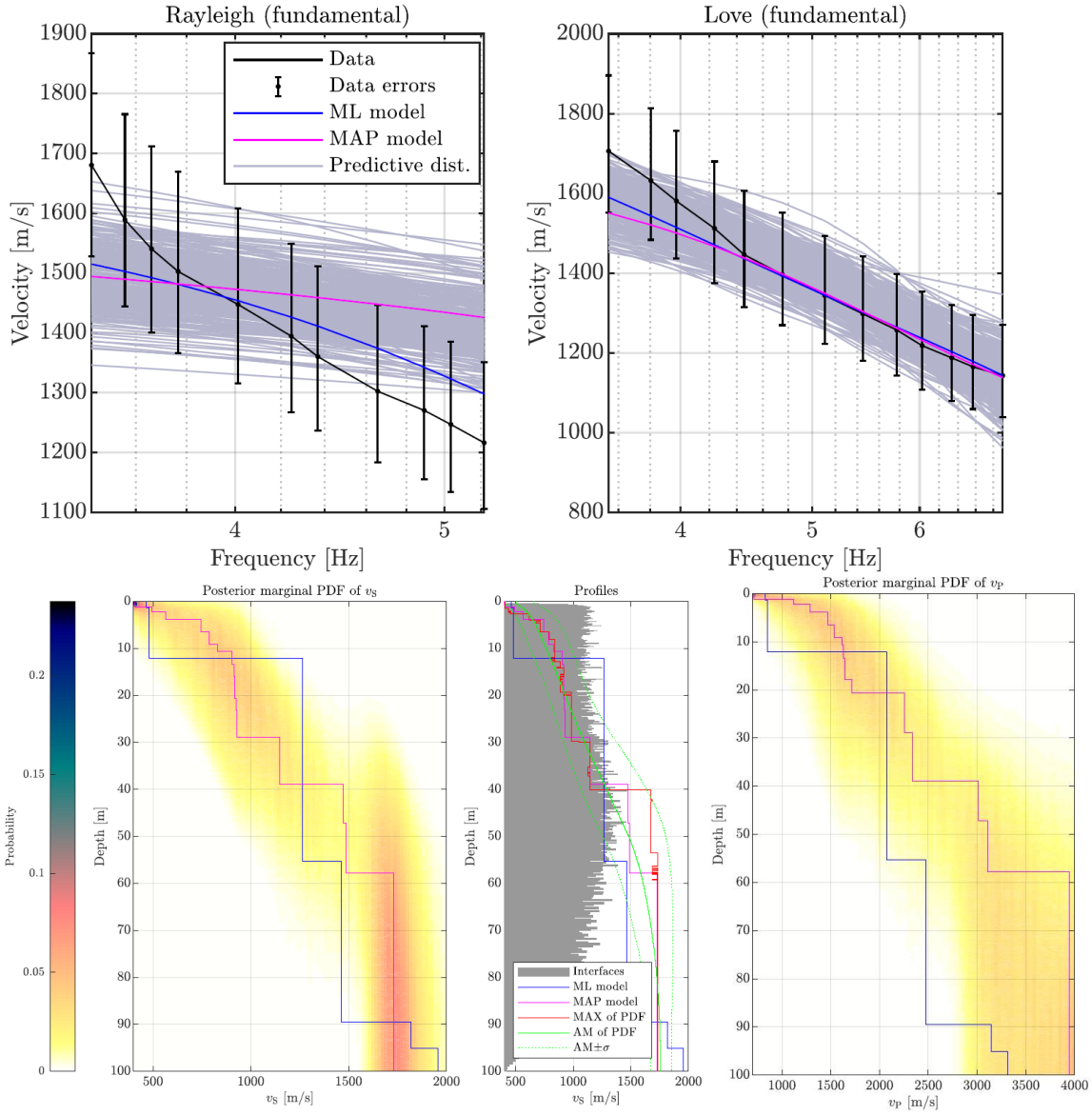

Figure S20. The fit of the modeled data to the experimental data (dispersion curves of analyzed modes R0 and L0) for array HEI100; grey curves represent 500 random models from the ensemble of solutions to show the scatter of possible inverse problem solutions with different misfit (i.e. the posterior predictive distribution); the black curve with the data errors represents the experimental data; the blue and purple curves are the ML and MAP models, respectively combined with S-wave (bottom left panel) and P-wave (bottom right panel) velocity profiles. The color represents the probability; the blue and purple curves are the ML and MAP models, respectively.

HEI200 R0L0 v.1

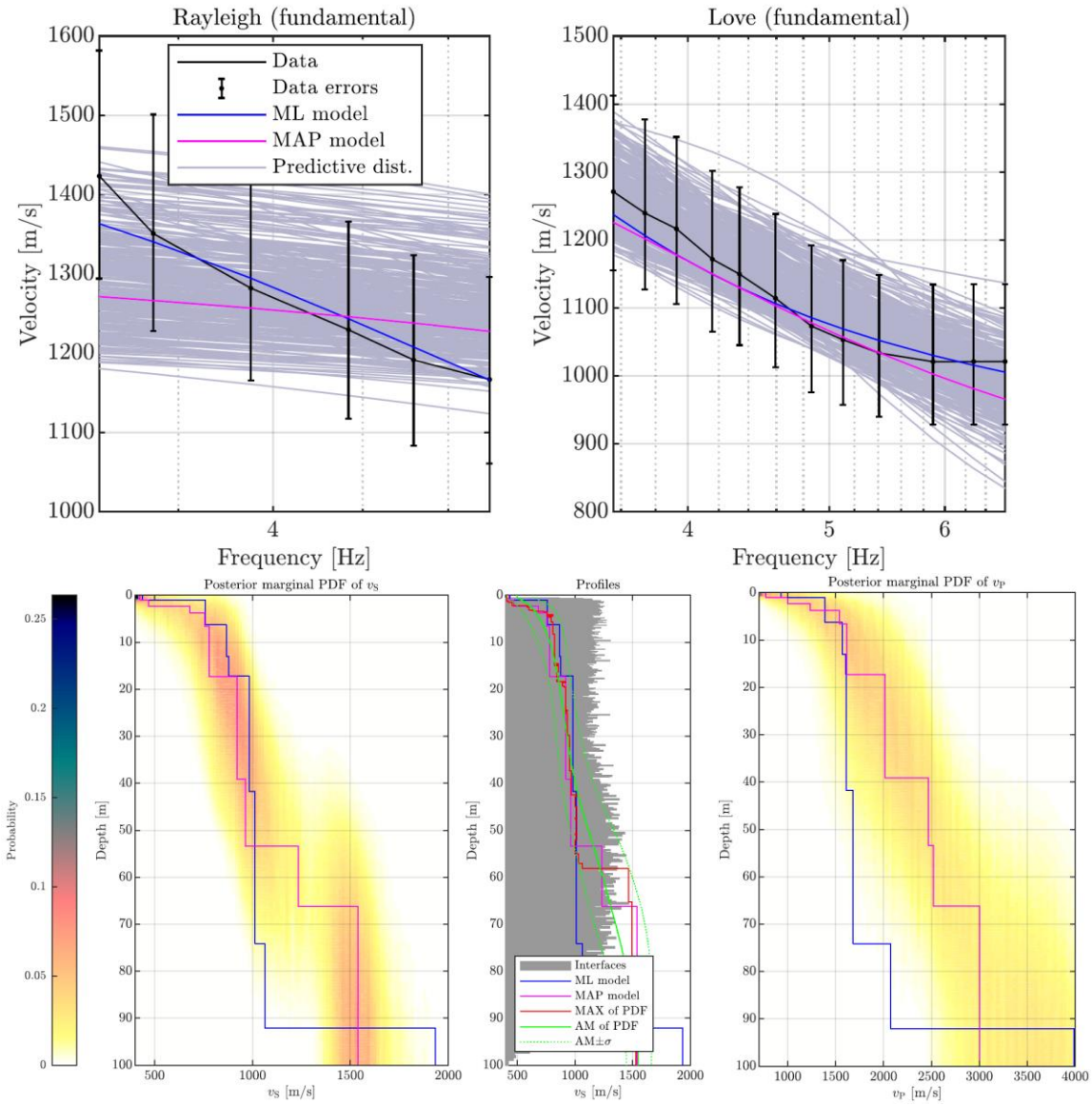

Figure S21. The fit of the modeled data to the experimental data (dispersion curves of analyzed modes R0 and L0 version 1) for array HEI200; grey curves represent 500 random models from the ensemble of solutions to show the scatter of possible inverse problem solutions with different misfit (i.e. the posterior predictive distribution); the black curve with the data errors represents the experimental data; the blue and purple curves are the ML and MAP models, respectively combined with S-wave (bottom left panel) and P-wave (bottom right panel) velocity profiles. The color represents the probability; the blue and purple curves are the ML and MAP models, respectively.

HEI200 R0L0 v.2

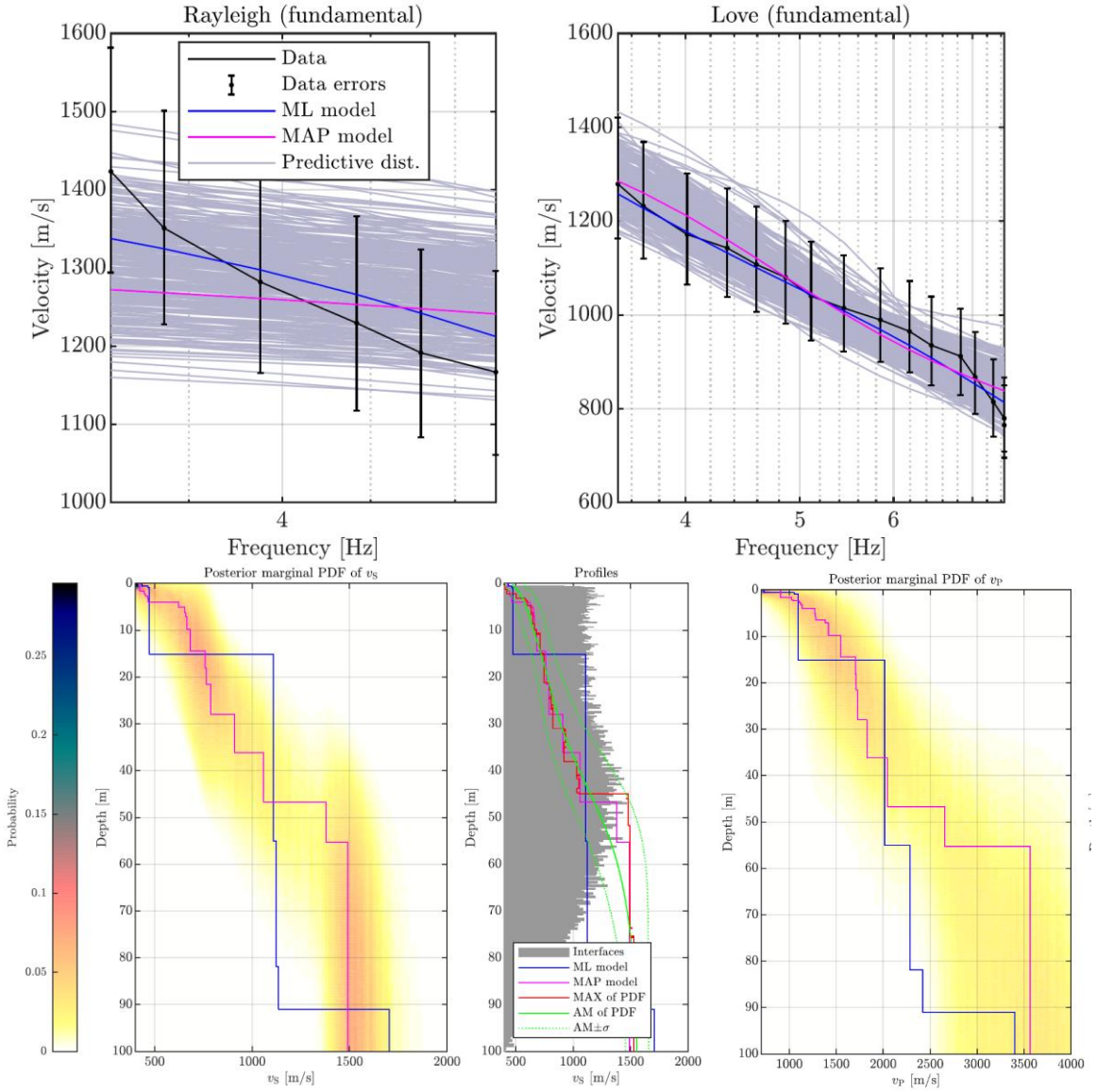

Figure S22. The fit of the modeled data to the experimental data (dispersion curves of analyzed modes R0 and L0 version 2) for array HEI200, with the love wave interpreted differently in the dispersion curve; grey curves represent 500 random models from the ensemble of solutions to show the scatter of possible inverse problem solutions with different misfit (i.e. the posterior predictive distribution); the black curve with the data errors represents the experimental data; the blue and purple curves are the ML and MAP models, respectively combined with S-wave (bottom left panel) and P-wave (bottom right panel) velocity profiles. The color represents the probability; the blue and purple curves are the ML and MAP models, respectively.

HEI300 R0 SP03N

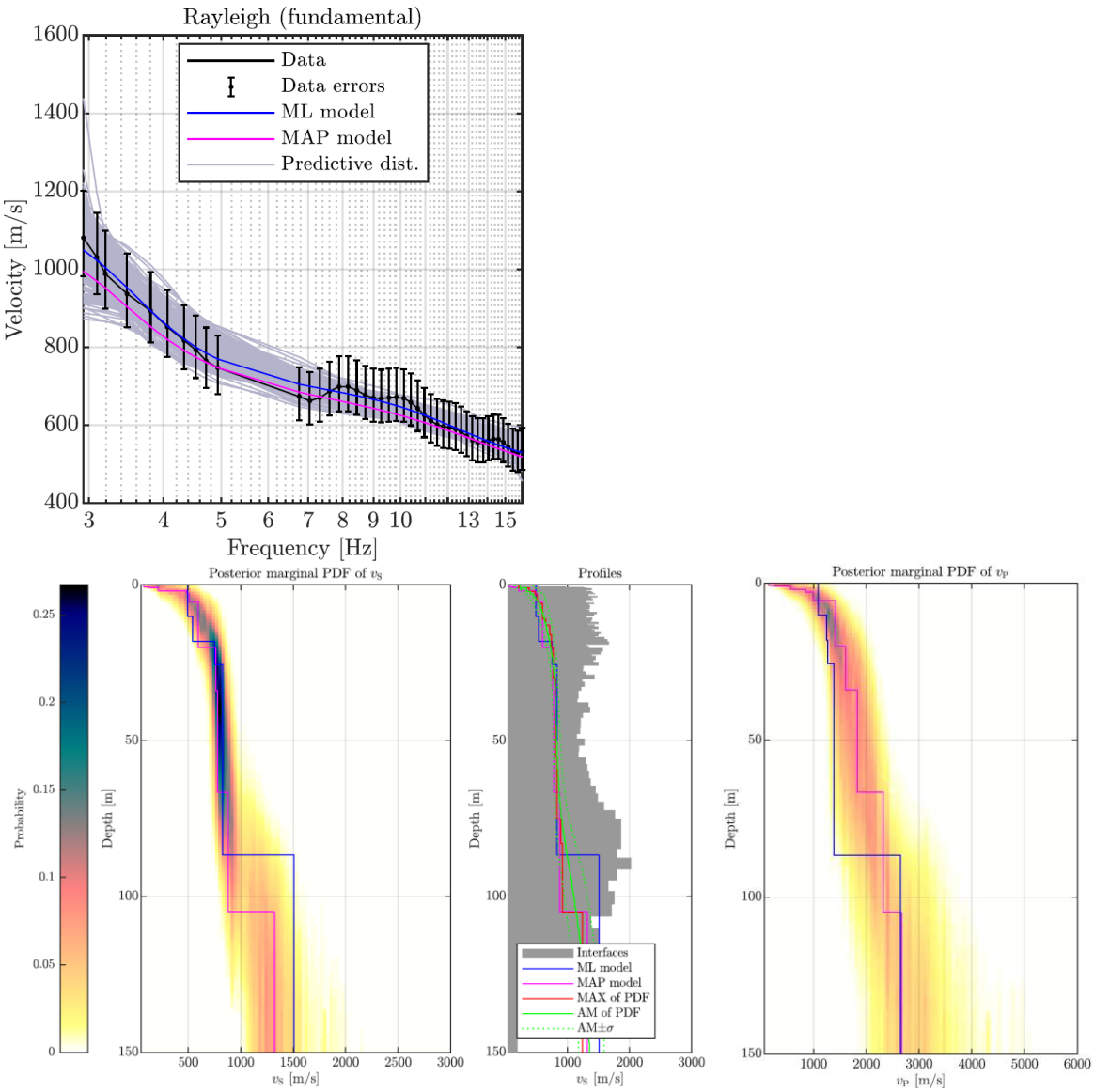

Figure S23. The fit of the modeled data to the experimental data (dispersion curves of analyzed mode R0 for array HEI300); grey curves represent 500 random models from the ensemble of solutions to show the scatter of possible inverse problem solutions with different misfit (i.e. the posterior predictive distribution); the black curve with the data errors represents the experimental data; the blue and purple curves are the ML and MAP models, respectively combined with S-wave (bottom left panel) and P-wave (bottom right panel) velocity profiles. The color represents the probability; the blue and purple curves are the ML and MAP models, respectively.

HEI300 R0R1 SP03N

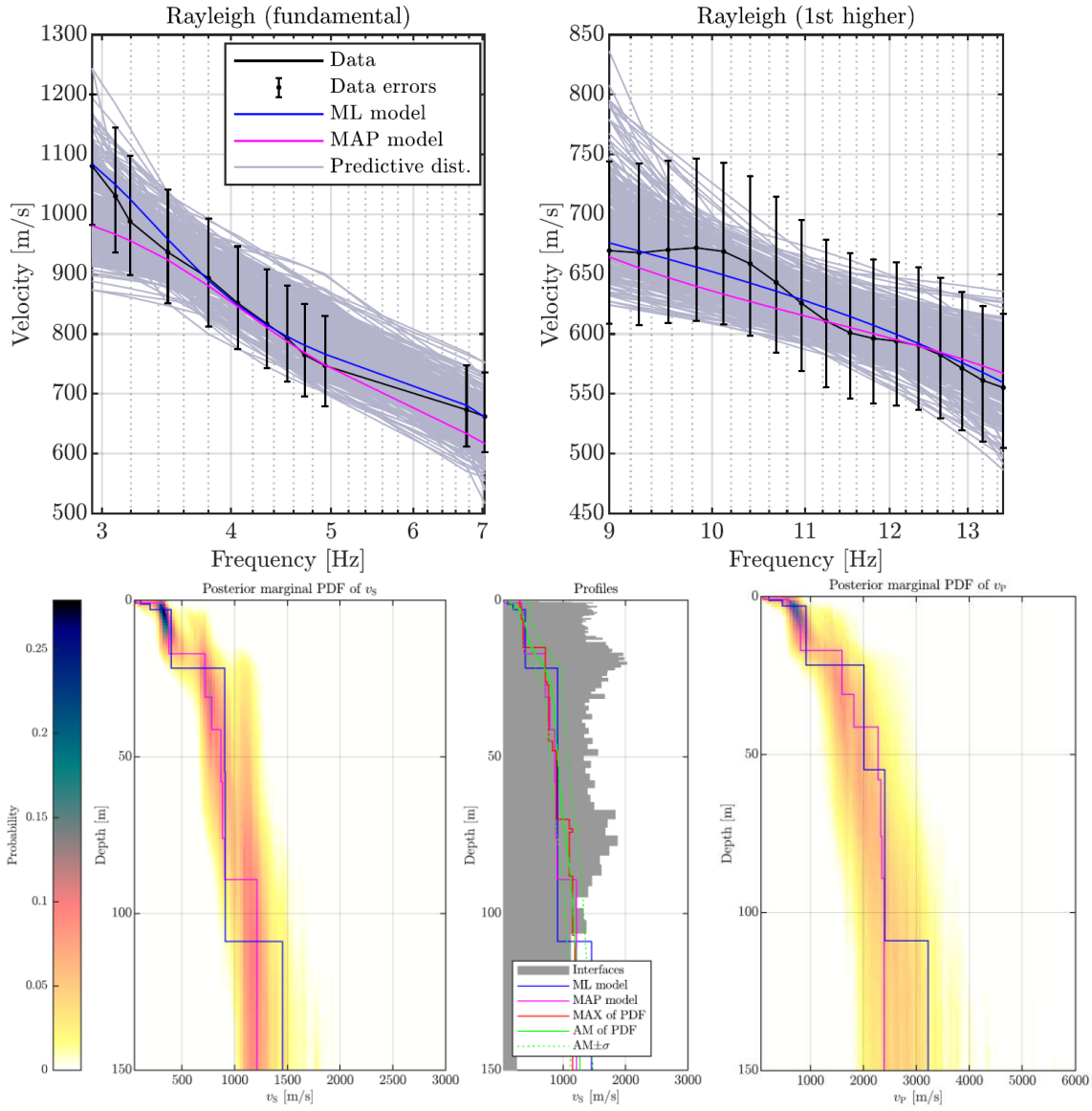

Figure S24. The fit of the modeled data to the experimental data (dispersion curves of analyzed modes R0 and R1) for array HEI300; grey curves represent 500 random models from the ensemble of solutions to show the scatter of possible inverse problem solutions with different misfit (i.e. the posterior predictive distribution); the black curve with the data errors represents the experimental data; the blue and purple curves are the ML and MAP models, respectively combined with S-wave (bottom left panel) and P-wave (bottom right panel) velocity profiles. The color represents the probability; the blue and purple curves are the ML and MAP models, respectively.

HEI400 R0L0

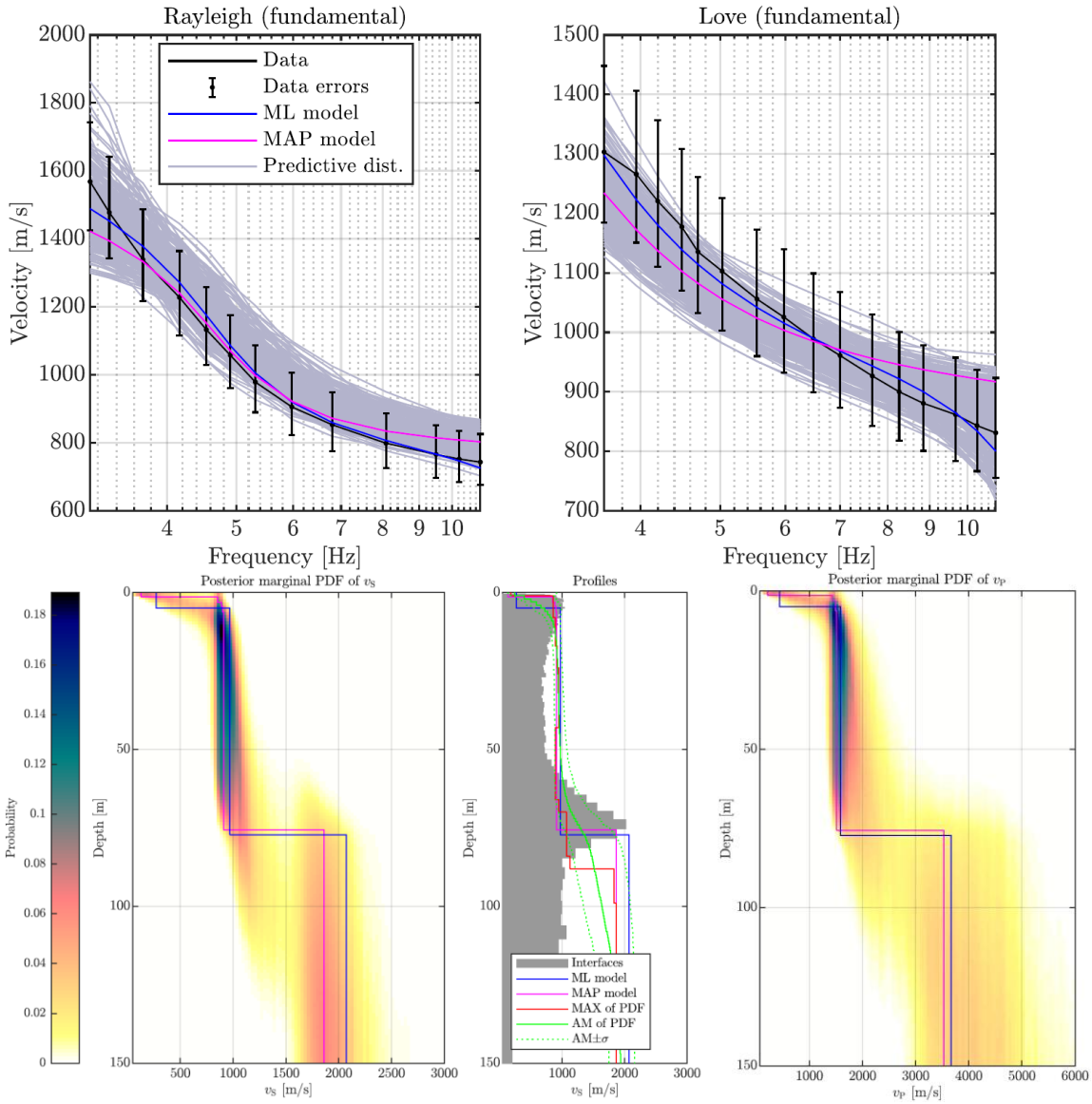

Figure S25. The fit of the modeled data to the experimental data (dispersion curves of analyzed modes R0 and L0) for array HEI400; grey curves represent 500 random models from the ensemble of solutions to show the scatter of possible inverse problem solutions with different misfit (i.e. the posterior predictive distribution); the black curve with the data errors represents the experimental data; the blue and purple curves are the ML and MAP models, respectively combined with S-wave (bottom left panel) and P-wave (bottom right panel) velocity profiles. The color represents the probability; the blue and purple curves are the ML and MAP models, respectively.

HEI400 R0R1

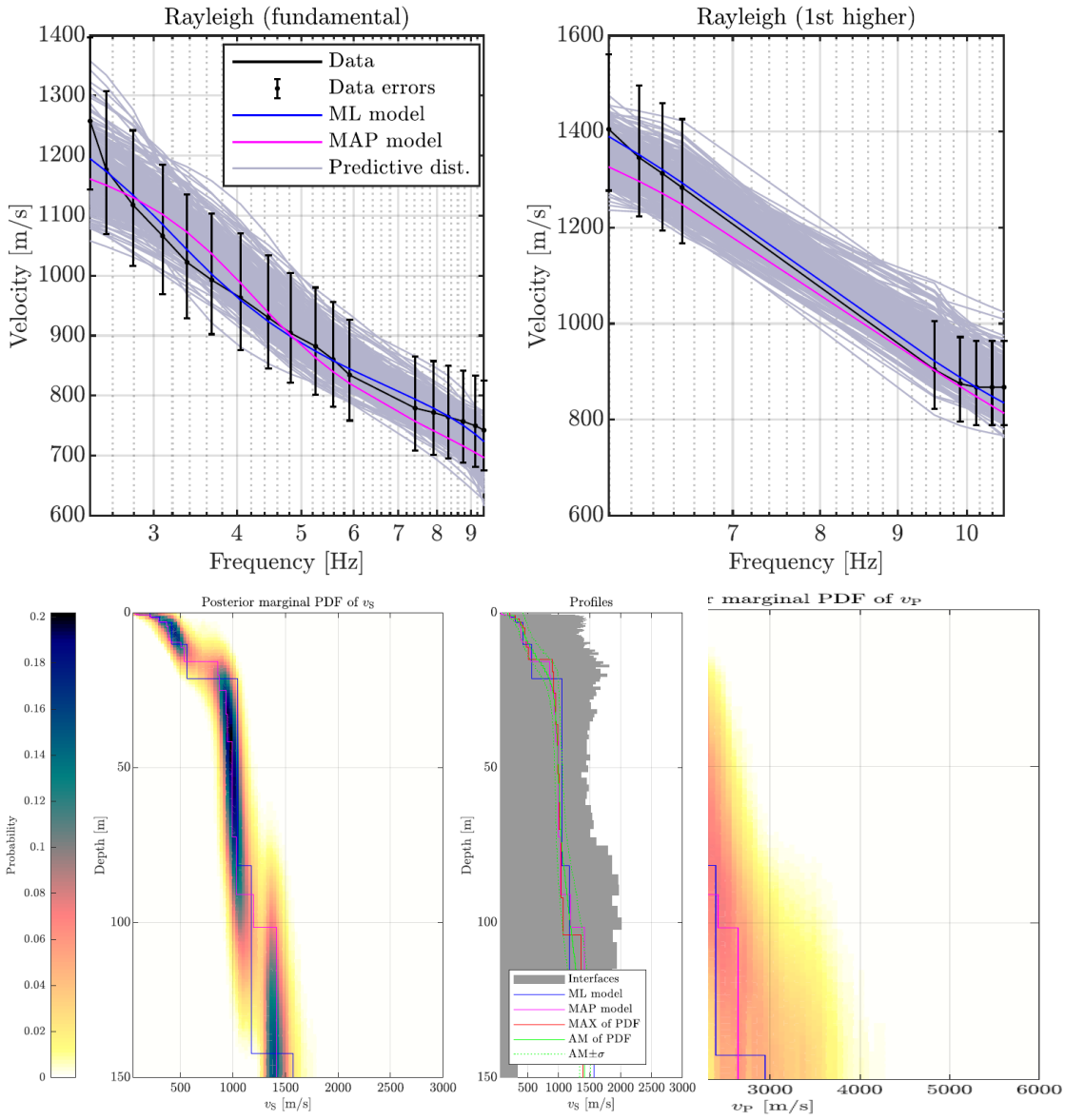

Figure S26. The fit of the modeled data to the experimental data (dispersion curves of analyzed modes R0 and R1) for array HEI400; grey curves represent 500 random models from the ensemble of solutions to show the scatter of possible inverse problem solutions with different misfit (i.e. the posterior predictive distribution); the black curve with the data errors represents the experimental data; the blue and purple curves are the ML and MAP models, respectively combined with S-wave (bottom left panel) and P-wave (bottom right panel) velocity profiles. The color represents the probability; the blue and purple curves are the ML and MAP models, respectively.

HEI400 R0R1R2

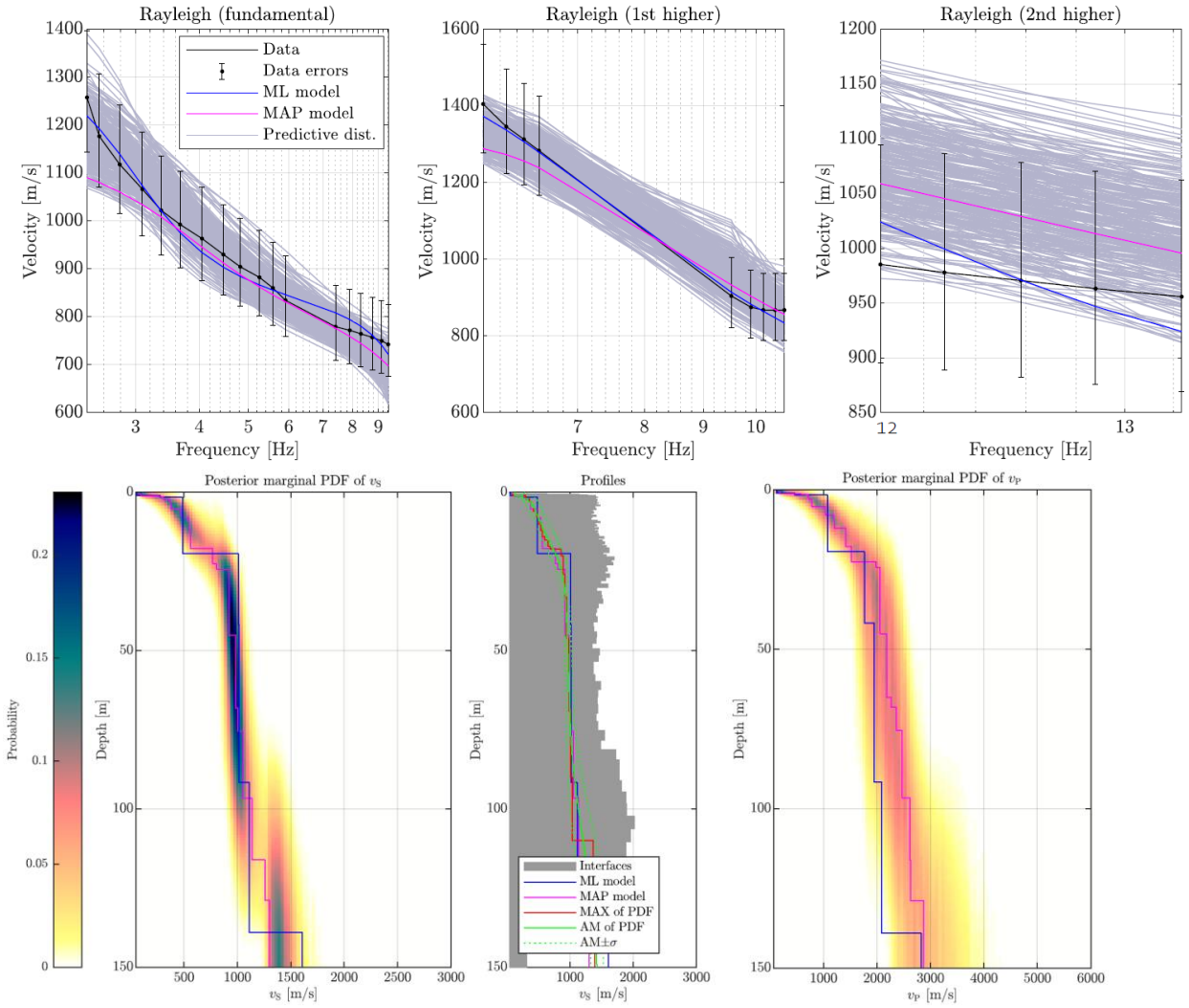

Figure S27. The fit of the modeled data to the experimental data (dispersion curves of analyzed modes R0, R1, and R2) for array HEI400; grey curves represent 500 random models from the ensemble of solutions to show the scatter of possible inverse problem solutions with different misfit (i.e. the posterior predictive distribution); the black curve with the data errors represents the experimental data; the blue and purple curves are the ML and MAP models, respectively combined with S-wave (bottom left panel) and P-wave (bottom right panel) velocity profiles. The color represents the probability; the blue and purple curves are the ML and MAP models, respectively.

HEI500 R0

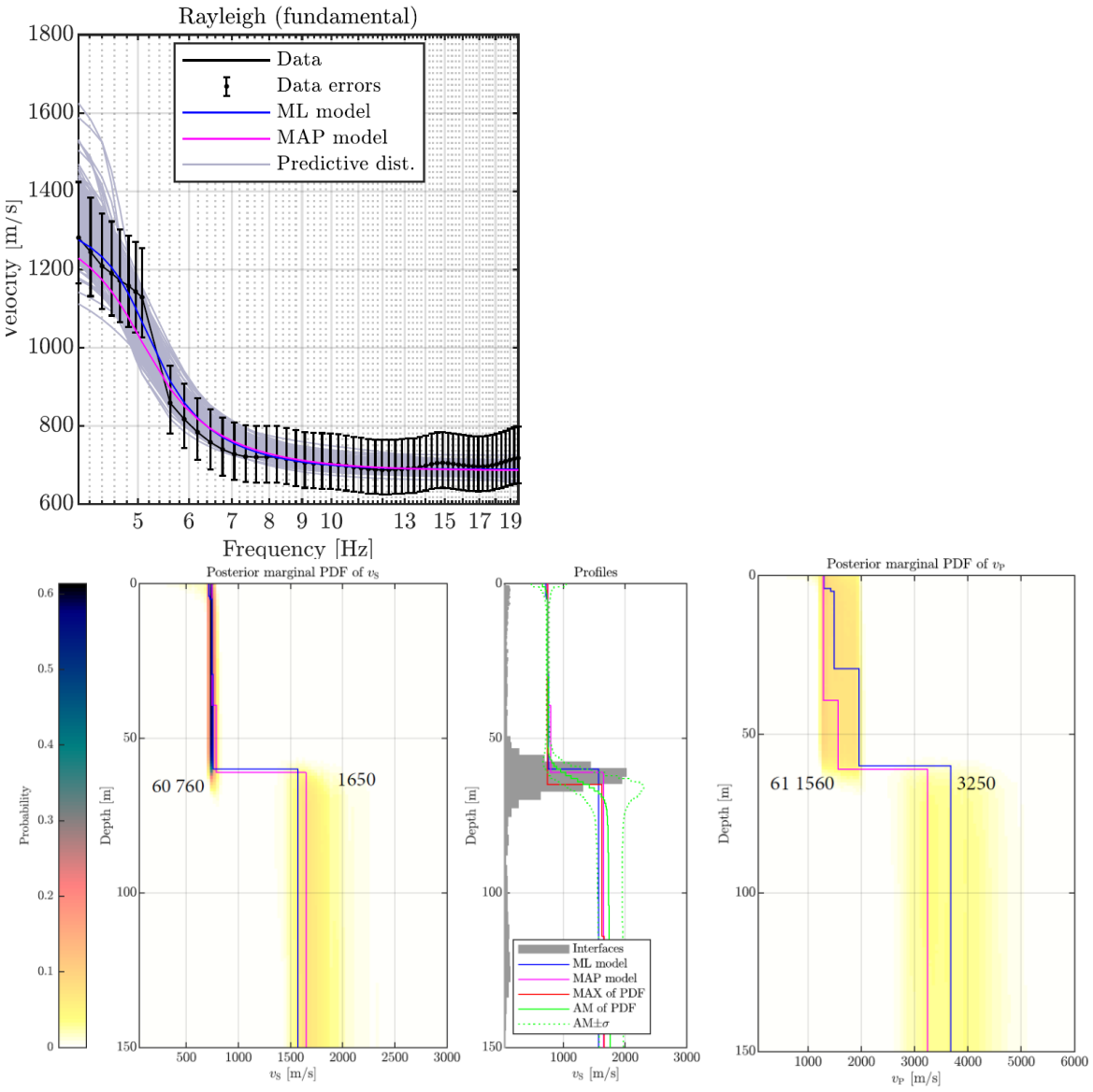

Figure S28. The fit of the modeled data to the experimental data (dispersion curves of analyzed modes R0) for array HEI500; grey curves represent 500 random models from the ensemble of solutions to show the scatter of possible inverse problem solutions with different misfit (i.e. the posterior predictive distribution); the black curve with the data errors represents the experimental data; the blue and purple curves are the ML and MAP models, respectively combined with S-wave (bottom left panel) and P-wave (bottom right panel) velocity profiles. The color represents the probability; the blue and purple curves are the ML and MAP models, respectively.

HEI500 R0R1

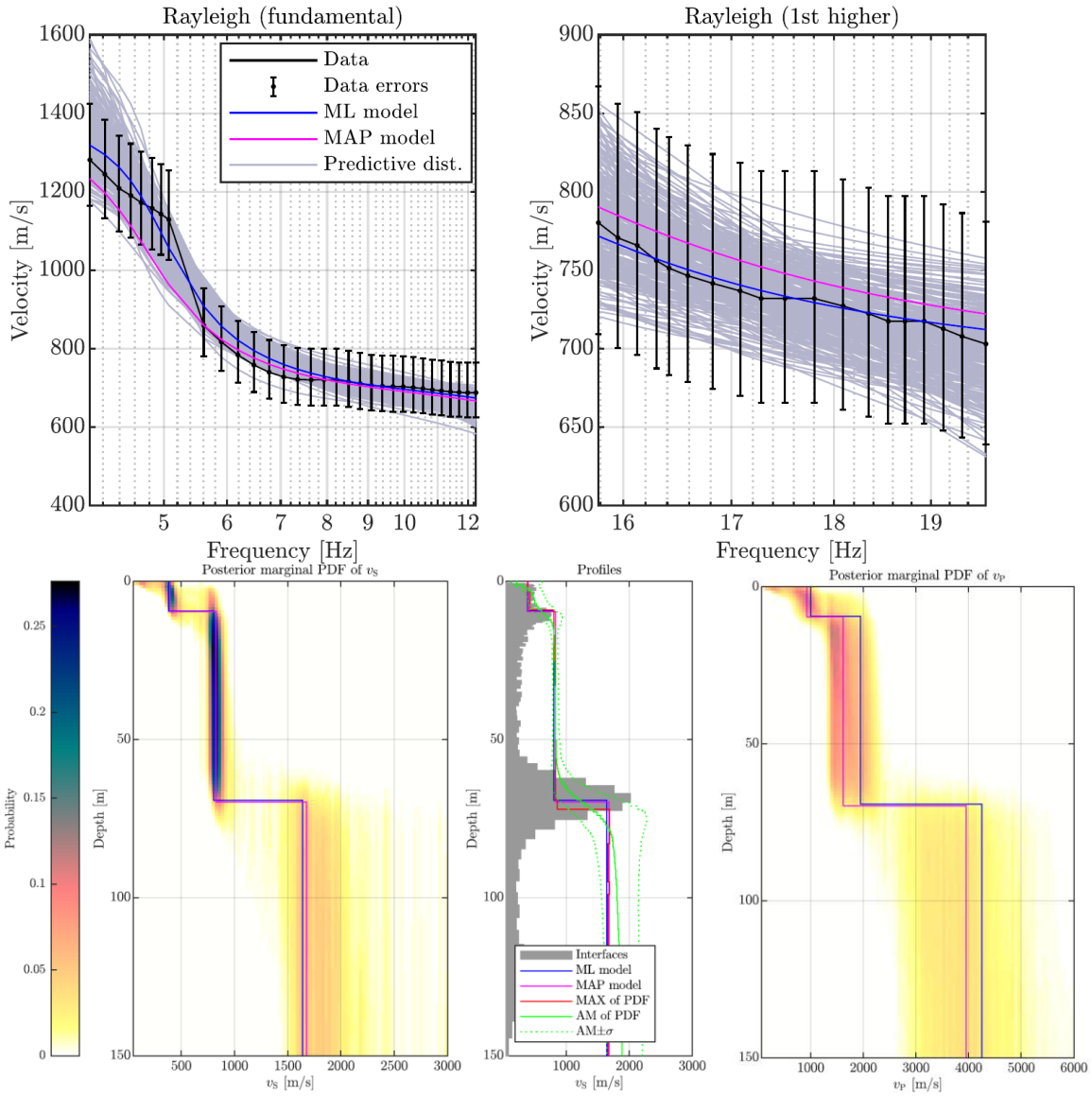

Figure S29. The fit of the modeled data to the experimental data (dispersion curves of analyzed modes R0 and R1) for array HEI500; grey curves represent 500 random models from the ensemble of solutions to show the scatter of possible inverse problem solutions with different misfit (i.e. the posterior predictive distribution); the black curve with the data errors represents the experimental data; the blue and purple curves are the ML and MAP models, respectively combined with S-wave (bottom left panel) and P-wave (bottom right panel) velocity profiles. The color represents the probability; the blue and purple curves are the ML and MAP models, respectively.

HEI500 R0R1R2

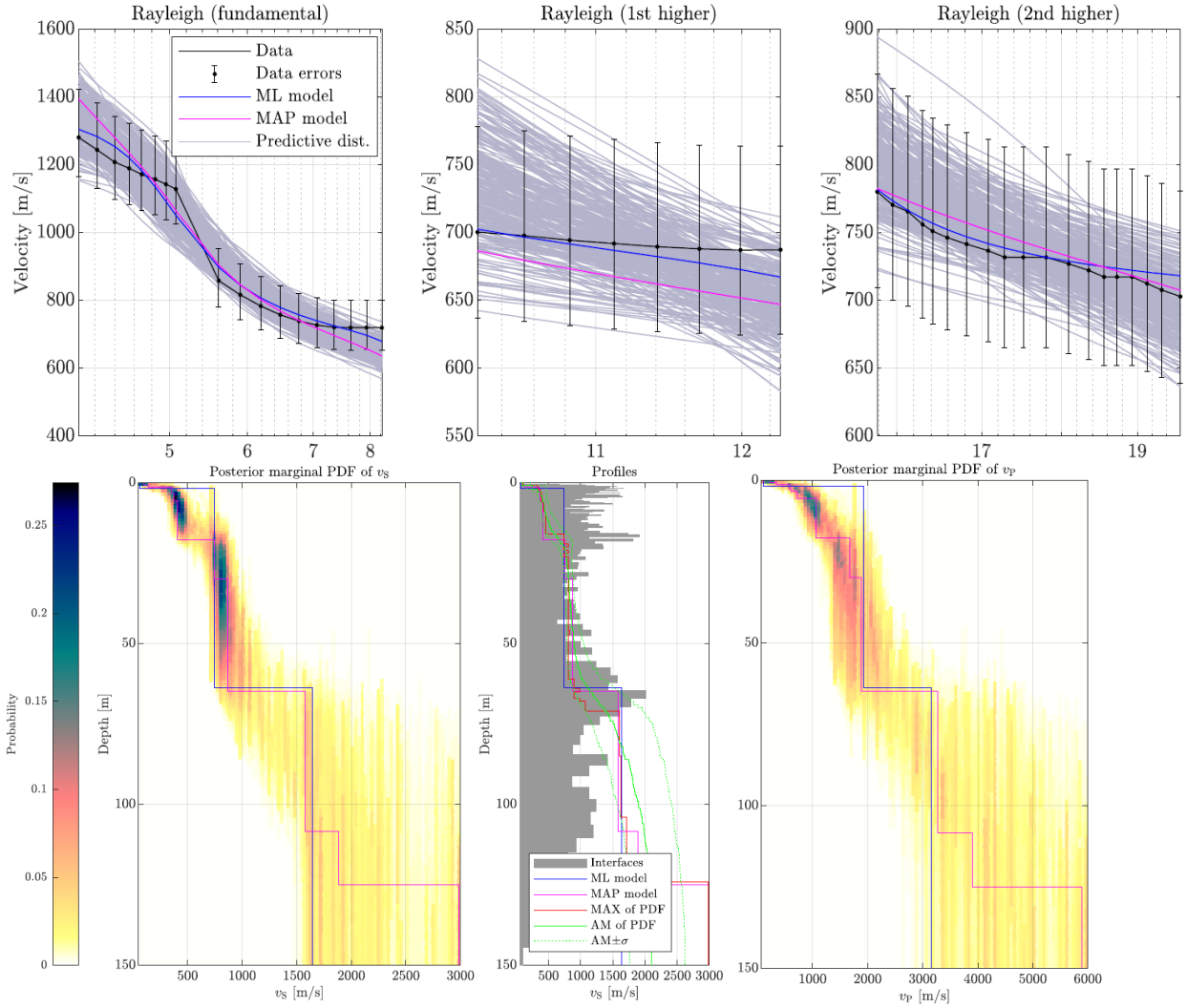

Figure S30. The fit of the modeled data to the experimental data (dispersion curves of analyzed modes R0, R1, and R2) for array HEI500; grey curves represent 500 random models from the ensemble of solutions to show the scatter of possible inverse problem solutions with different misfit (i.e. the posterior predictive distribution); the black curve with the data errors represents the experimental data; the blue and purple curves are the ML and MAP models, respectively combined with S-wave (bottom left panel) and P-wave (bottom right panel) velocity profiles. The color represents the probability; the blue and purple curves are the ML and MAP models, respectively**.**